Can machine-learning algorithms improve upon classical palaeoenvironmental reconstruction models?

Peng Sun[1], Philip. B. Holden[2], and H. John B. Birks[3,4]

[1]Institute of Environmental Sciences (CML), Leiden University, 2333 CC Leiden, the Netherlands
[2]Environment, Earth and Ecosystem Sciences, The Open University, Walton Hall, Milton Keynes, MK7 6AA, UK
[3]Department of Biological Sciences and Bjerknes Centre for Climate Research, University of Bergen, PO Box 7803, Bergen N-5020, Norway [4]Environmental Change Research Centre, University College London, London WC1 6BT, UK

Correspondence to: Philip B. Holden (philip.holden@open.ac.uk)

Abstract. Classical palaeoenvironmental reconstruction models often incorporate biological ideas and commonly assume that the taxa comprising a fossil assemblage exhibit unimodal response functions of the environmental variable of interest. In contrast, machine-learning approaches do not rely upon any biological assumptions, but instead need training with large data-sets to extract some understanding of the relationships between biological assemblages and their environment. To explore the relative merits of these two approaches, we have developed a two-layered machine learning reconstruction model MEMLM (Multi Ensemble Machine Learning Model). The first layer applies three different ensemble machine-learning models (random forests, extra random trees, and lightGBM), trained on the modern taxon assemblage and associated environmental data to make reconstructions based on the three different models, while the second layer uses multiple linear regression to integrate these three reconstructions into a consensus reconstruction. We considered three versions of the model: 1) a standard version of MEMLM, which uses only taxon abundance data, 2) MEMLMe, which uses only dimensionally reduced assemblage information, using a natural language-processing model (GloVe) to detect associations between taxa across the training data-set, and 3) MEMLMc which incorporates both raw taxon abundance and dimensionally reduced summary (GloVe) data. We trained these MEMLM model variants with three high quality diatom and pollen training sets and compared their reconstruction performance with three weighted averaging (WA) approaches (WA-Cla, classical deshrinking; WA-Inv, inverse deshrinking; and WA-PLS, partial least squares). In general, the MEMLM approaches, even when trained on only embedded assemblage data, performed substantially better than the WA approaches under cross-validation in the larger data-sets. When applied to fossil data, MEMLM variants sometimes generated qualitatively different palaeoenvironmental reconstructions from each other and from reconstructions based on WA approaches. We applied a statistical significance test to all the reconstructions. This successfully identified each incidence where the reconstruction is not robust with respect to the model choice. We found that machine-learning approaches could outperform classical approaches, but could sometimes fail badly, despite showing high performance under cross-validation, likely indicating problems when extrapolation occurs. We found that the classical approaches are generally more robust, although they could also generate reconstructions which have modest statistical significance, and therefore may be unreliable. We conclude that cross-validation is not a sufficient measure of transfer-function

Deleted:
Deleted:
Deleted: We
Deleted:
Deleted: of
Deleted: ,
Deleted: consider
Deleted: A
Deleted: embedded
Deleted:
Deleted: GLOVE
Deleted: assemblage data
Deleted: train
Deleted: compare
Deleted: of
Deleted: (
Deleted:),
Deleted: (
Deleted:)
Deleted: (
Deleted: perform
Deleted: However, when
Deleted: and WA approaches
Deleted: generate
Deleted: .
Deleted: find
Deleted:
Deleted: can
Deleted: can
Deleted: catastrophically
Deleted: find
Deleted: can

performance, and we recommend that the results of statistical significance tests are provided alongside the down-core reconstructions based on fossil assemblages.

1 INTRODUCTION

The distribution and abundance of taxa are interrelated with the environment (Ovaskainen et al., 2017). By considering environmental variability across space instead of through *time*, the palaeoenvironment can be reconstructed by applying modern taxon-environment relationships to the fossil record (e.g. Battarbee et al., 2005; Cleator et al., 2020; Turner et al., 2020).

With the development of palaeoecological research, large training data-sets for environmental reconstruction have been compiled in recent years. (e.g. Harrison, 2019a; Bush et al., 2021). Data assimilation has long been a focus of Earth science and ecology, and the integration of larger data-sets provides more comprehensive training information (e.g. Christin et al., 2019; de la Houssaye et al., 2019; Bush et al., 2021). For large data-sets, machine-learning methods have strong advantages and may be appropriate to extract the non-linear relationships between taxon compositional information and the environment, and to integrate a variety of sources of data (e.g. Helama et al., 2009; Aguirre-Gutierrez et al., 2021; Wei et al., 2021b).

In recent years, machine learning has been applied to a wide range of applications in palaeoecology (Hais et al., 2015; Jordan et al., 2016). Wei et al. (2021b) reconstructed palaeoclimate using five different machine-learning methods based on digital leaf physiognomic data and integrated the predictions by averaging. Hais et al. (2015) predicted the Pleistocene biota distributions in palaeoclimate using machine learning. Huang et al. (2020) used one series of palaeoclimate sequences to predict the climate in another period. These studies show that machine learning has strong versatility and effectiveness, and suggest it could be more widely applied.

Machine-learning approaches are not based upon any biological assumptions, which may weaken their performance relative to mathematically simpler classical approaches that do. For instance, weighted averaging (WA) approaches are based upon the simple but realistic assumption that taxa have a unimodal response to the environmental variable of interest (ter Braak and Barendregt, 1986). The absence of any such prior understanding is likely to place additional demands on the minimum adequate size of a modern training set. Moreover, it may weaken the ability of machine learning to operate under extrapolation, critically important when applying any reconstruction approach to past taxon assemblages that lack modern analogues. To address these questions, we have developed the Multi Ensemble Machine Learning Model (MEMLM) to apply in a systematic comparison with classical WA reconstruction approaches.

The benefit of machine learning lies in its robust data mining and information extraction capabilities, especially when applied to large data-sets. Data mining involves discovering patterns, trends, and correlations hidden within extensive data-sets. Information extraction, on the other hand, focuses on extracting insights from unstructured data, typically relying on Natural Language Processing and encoding techniques to understand and analyse semantic information embedded within unstructured

Formatted: Font colour: Auto
Formatted: Font colour: Black
Formatted: Font colour: Auto
Deleted: By using the concept
Deleted: *space instead*
Formatted: Font: Italic
Deleted: emerged
Deleted: 2019
Deleted: will provide
Deleted: 2020
Deleted:
Deleted: ,
Deleted: ,
Deleted: .,
Deleted:
Deleted: .,
Deleted: .,
Deleted: should
Deleted: However, machine
Deleted: do
Deleted: make
Deleted: apply
Deleted: informative
Deleted: is that it has strong

data. An associated problem is that when a sample size is limited, machine learning is more likely to learn the noise component and generate prediction errors due to over-fitting (Yeom et al., 2018; Syam and Kaul, 2021). This suggests that an ensemble learning method, which integrates models with potentially different biases, may improve the prediction performance (Wei et al., 2021b). Ensemble learning was developed to address these issues (Zhou, 2012) and is the motivation for the ensemble learning approach we present, namely the Multi Ensemble Machine Learning Model (MEMLM).

We build MEMLM from three different machine learning ensemble models of random forests, extra random trees, and lightGBM. We then combine these three models into a single consensus model which we treat as our 'best' machine-learning approach. Classical studies have integrated different ecological approaches by calculating the mean of their predictions (Norberg et al., 2019). An arithmetic mean gives equal weight to each model, even though the models may have different advantages in different applications (Schulte and Hinckley, 1985; Zhou, 2012). In MEMLM, we weight each model according to its predictive power under cross-validation.

Most classical models give equal weight to different taxa, which may reduce their prediction potential and smooth the reconstruction (e.g. Brooks and Birks, 2001; Heiri et al., 2003; Battarbee et al., 2005; Wei et al., 2021a). In WA-PLS (TWA-PLS), tolerance down-weighting can be applied to assign weights to each taxon in reconstructing the environment that depends upon the breadth of the taxon's environmental niche (Liu et al., 2020). Bayesian approaches such as BUMPER (Holden et al., 2017) are built on classical assumptions and are highly constrained by taxa with low environmental tolerances, especially when characterised with high confidence. In machine learning ensemble models, each taxon has a different predicted contribution which is used to weight its contribution to the ensemble.

We develop three versions of MEMLM; the standard version which only considers raw taxon abundance data; MEMLMe, which only uses dimensionally reduced (GloVe) assemblage data; and MEMLMc, which uses both. The motivation for the more complex versions is to explore whether considering known associations between taxa can improve the palaeoenvironmental reconstructions. For this, we use the natural language processing model GloVe (Pennington et al., 2014), which calculates the relationships between co-occurring words in the same sentence. GloVe is a form of dimension reduction which assigns vectors (also called embedding) to each word according to the word connection relationships, so that each sentence can be represented as a superposition of the word embeddings within that sentence. In taxon assemblages, there are analogous co-occurrence relationships between taxa which we hypothesise convey information on their ecological functioning. We therefore use GloVe to generate embedding vectors by considering the frequency of co-occurring taxon pairs across the training set. We then concatenate the embedding vectors of each sample to represent the assemblage.

2 MATERIALS AND METHODS

We apply MEMLM to high quality pollen and diatom training sets to generate down-core reconstructions. We calculate training set cross-validation metrics and we quantify the statistical significance and robustness of the core reconstructions. We

Deleted: ability.

Deleted: , however,

Deleted: reduce over-fitting errors (Legendre et al., 1997) and

Deleted: This

Deleted: reconstruction

Deleted: does not attribute weights

Deleted: Similarly, most

Deleted: do not consider different weights for

Deleted: Tolerance downweighted

Deleted:) makes it possible

Deleted: different

Deleted:), while

Deleted: ¶
In MEMLM, we apply both taxon weights and model weights. The first calculation layer applies three different machine learning ensemble models of random forests, extra random trees and lightGBM, trained on modern taxon assemblage and environmental data. In these

Deleted: The three reconstructions are then integrated into a consensus reconstruction using a weak learning algorithm which weights each model according to its predictive power under cross-validation.

Deleted: includes encoded

Deleted: information

Deleted: includes

Deleted: (NLP)

Deleted: GLOVE

Deleted: GLOVE

Deleted: environmental

Deleted: GLOVE

Deleted: the

Deleted: different taxa in different samples based on assemblage information and

Deleted: to integrate

Deleted: embeddings within

Deleted:

Deleted: We apply MEMLM to high quality pollen and diatom training sets to generate down-core reconstructions. We calculate training set cross-validation metrics and we quantify the statistical significance and robustness of the core reconstructions. We compare these performance metrics with those of classical WA approaches to evaluate whether, and under what circumstances, machine lear ... [1]

Formatted: Font colour: Auto

Formatted: Font colour: Black

Formatted: Font colour: Auto

compare these performance metrics with those of classical WA approaches to evaluate whether, and under what circumstances, machine-learning approaches might be able to outperform classical WA-based reconstruction approaches.

Deleted:

2.1. MEMLM

MEMLM combines a series of modules (Figure 1). In this section, we introduce the functions of each module and the data processing approach. There are three model variants (MEMLM, MEMLMe, and MEMLMc), each of which takes different inputs (Figure 1), which is the only difference in their construction. The scientific motivation for the three variants is to explore i) whether machine learning decision trees can extract all useful information (MEMLM), or, if not, ii) whether GloVe can improve this (MEMLMc) and iii) whether GloVe alone is sufficient to encode assemblage data (MEMLMe). Each variant is built using the same three machine-learning approaches (random forests, extra random trees, and lightGBM), which are combined into a single consensus reconstruction model for each routes.

Formatted: Font: 9 pt, Bold

Formatted: Font: 10 pt, Not Bold

Formatted: Font: 9 pt, Bold

Formatted: Font: 10 pt, Not Bold

Deleted: routes.

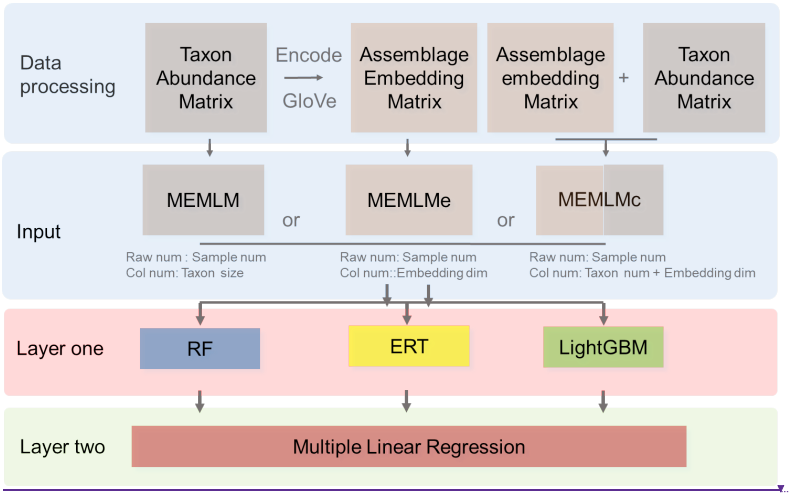

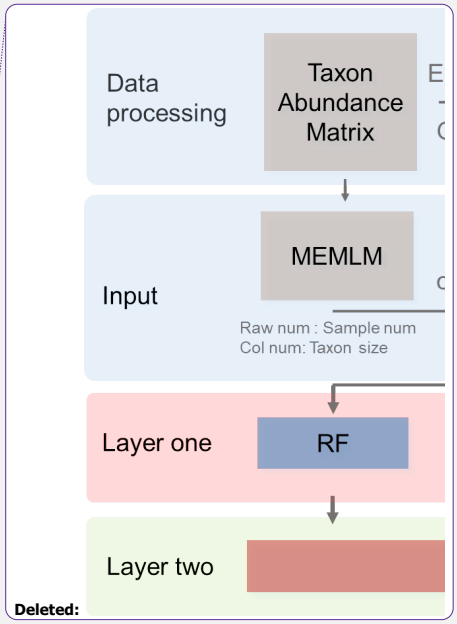

Deleted:

Figure 1: Multi Ensemble Machine Learning Model (MEMLM) model framework. MEMLM has a modular building block architecture so that components can be easily changed. Raw num and Col num are the number of rows and columns in the input matrix; dim is the number of dimensions.

2.1.1. First layer

The input data comprise environmental data together with either the taxon abundance matrix, the assemblage embedding matrix, or both matrices (see section 2.2.3 for a description of the embedding algorithm to develop the assemblage matrix). We apply three ensemble machine-learning models to derive the mapping between taxon composition information and environmental factors:

(1) Random forests (RF) is an ensemble machine-learning model composed of multiple decision trees. The overall model framework is determined based on the predictive power of each decision tree applied to the training data-set under bootstrapping. Individual decision trees with better predictive performance are allocated higher weights, and the 'forest' integrates the weighted result from each tree (Liaw and Wiener, 2002).

(2) Extra Random Tree (ERT) is similar to RF, except that it uses the entire data-set rather than a bootstrapped subset (Geurts et al., 2006).

(3) LightGBM is based on the Gradient Boosting Decision Tree. This also integrates decision trees, but LightGBM differs by applying 'gradient boosting' to add new trees, building each new model on the residuals of the previous model to improve the prediction. It has the ability to merge sparse data-sets to increase computational efficiency (Friedman, 2001; Ke et al., 2017).

2.1.2 Second layer (consensus reconstruction)

It is possible to improve prediction performance by integrating the prediction of multiple models into a consensus reconstruction (Yeom et al., 2018; Syam and Kaul, 2021). Averaging is widely used to integrate the output prediction of multiple models. However, the integration weight of each model is the same under averaging. MEMLM applies multiple linear regression to allocate an integration weight to each model rather than attaching each model with the same weight. The consensus reconstruction is derived as follows. First, the three upstream models are applied to reconstruct the training data-set under five-fold cross-validation. We then build a multiple linear regression model to fit the reconstructed values to the actual value in the training set. This approach is designed to avoid the risk of over-fitting while reducing the impact of low-performance models on the consensus reconstruction. Exploratory analysis applied to the NIMBIOS data-set, building models for each of 18 environment attributes, demonstrated that the multiple linear regression approach reduced the root mean square error of prediction (RMSEP) relative to the individual reconstructions by an average of 8% (Table A1). A consensus reconstruction based on the mean of the three ensemble approaches also improved predictive power but reduced the cross-validated RMSEP errors relative to the individual reconstructions by an average of 5%. We note that while the stacking approach reduces RMSEP by typically 8%, we show in Section 3.1 and Table 1 that such improvements are modest relative to the improvements from the machine learning itself. Weights of the linear models of MEMLM, MEMLMe, and MEMLMc based on the three training sets are provided in Table A2.

Deleted:

Deleted:

Deleted: ET

Deleted:

Deleted: 2017

Deleted: squared

2.1.3 Embedding

The GloVe algorithm (Pennington et al., 2014) is a very widely used linguistic dimensional reduction approach. It uses co-occurrences of words in phrases to characterise numerically their meaning. In formal terms, GloVe is a row-column bilinear model of the form $r_i + c_k + R_i \times C_j$, least-squared fitted to the log-transformed co-occurrence matrix derived from the primary data. GloVe is thereby very close to unconstrained ordination models used in ecology except for the transformation to co-occurrences (ter Braak, 1988, ter Braak and te Beest, 2022).

In GloVe, words are represented as vectors in high dimensional space, where each dimension captures an aspect of meaning so that in this space words that have similar meanings are located near to each other. To illustrate, in word vector space, we would expect the difference vectors $\boldsymbol{queen - king}$ and $\boldsymbol{girl - boy}$ to be similar, as they both reflect only a change of gender, with other dimensions of meaning (species, age, social status etc) constant. Embedding reduces the dimensionality of a vocabulary from tens of thousands of words to hundreds of similar meaning dimensions, known as features.

In ecology, co-existence among taxa can reflect characteristics of the environment (Ovaskainen et al., 2017). We hypothesise that taxa within an assemblage have relationships that are analogous to words within a phrase, so that in the feature space of ecological 'meaning' the vectorial representation of a taxon describes its ecological function. We apply GloVe to ecological assemblages. Instead of analysing co-occurrences of words within phrases, we analyse co-occurrences of taxa within assemblages. The objective is to extract ecological information by associating taxa with their ecosystem functioning.

The GloVe algorithm is fully detailed in Pennington et al. (2014), and here we introduce the underlying philosophy and illustrate it in the context of ecological functioning. Consider P_{ij} the conditional probability that taxon j appears in the same assemblage as taxon i:

$$P_{ij} = P(j|i) = X_{ij}/X_i \quad (1)$$

where X_{ij} is the number of assemblages which contain both taxa i and j, and X_i is the number of assemblages containing taxon i. This probability does not necessarily indicate the strength of the relationship. Consider, for instance, that a high value may simply reflect that taxon j is common and therefore provides little information about the environment.

To determine associative relationships, GloVe considers the ratio P_{ik}/P_{jk} where taxon k is some probe taxon used to differentiate the ecological functioning of i and j. If taxon k has a strong association with taxon i but not with taxon j then $P_{ik}/P_{jk} \gg 1$. However, if all three taxa are either commonly found together or have no relationship (i.e. low but random co-occurrence) between each other, $P_{ik}/P_{jk} \sim 1$, indicating that taxon k provides very little information to help distinguish the ecological functions of i and j. The value of P_{ik}/P_{jk} can therefore inform us about the direction of difference vector $i - j$. GloVe is trained on assemblages to map taxa onto vectors in feature space, so that the assemblages can be described as linear combinations of the features. For application to MEMLMc, the feature matrices are provided together with the raw taxon count data to provide richer training data for the ensemble learning algorithms.

Deleted: GLOVE

Deleted: Words

Deleted: Legendre et al., 1997;

Deleted: GLOVE

Deleted: GLOVE

Deleted: GLOVE

Deleted:

Deleted: GLOVE

Formatted: Font: Not Bold

We note that while the GloVe algorithm closely resembles unconstrained ordination, GloVe emphasises semantics, seeking dimensions which convey meaning and which have relatively similar importance. This contrasts with unconstrained ordination, which focuses on the explanation of variance and dimension ordering. By focusing on semantics, we expect that GloVe will provide more interpretability than traditional dimensionality reduction methods.

2.2. Assemblage data

For model training purposes we use two large pollen data-sets, SMPDSV1 (Harrison, 2019a) and NIMBIOS (Bush et al., 2021), and the smaller diatom SWAP data-set (Stevenson et al., 1991). To demonstrate the palaeoenvironment reconstructions of each model, we apply i) SWAP to reconstruct lake-water pH from diatoms in a core from The Round Loch of Glenhead (RLGH) (Allott et al., 1992, Jones et al., 1989), ii) SMPDSV1 to reconstruct mean temperature of the coldest month (MTCO) from pollen in the Villarquemado core (Harrison, 2019a, Harrison, 2019b), and iii) NIMBIOS to reconstruct the mean annual temperature (MAT) from pollen in the Consuelo (Urrego et al., 2010) and Llaviucu (Steinitz-Kannan et al., 1983, Colinvaux et al., 1988) cores.

Deleted: apply
Deleted: 2019
Deleted: 2020
Deleted: In order to
Deleted: 2019
Deleted: average

2.2.1. Training data-sets

SWAP: The SWAP training set (Stevenson et al., 1991) was developed as part of an international scientific effort directed at establishing and understanding the impacts of acid rain on freshwaters. It includes relative abundance data for 277 diatom taxa from 167 modern samples with clear identification criteria standards (Birks et al., 1990). We apply these data to reconstruct lake-water pH.

The NIMBIOS data-set (Bush et al. 2020), includes samples from 636 neotropical locations with various habitat types. There are 533 pollen types (some taxa can only be identified to family level), ranging from soil samples to mud-water interface samples from lakes. We use it to reconstruct mean annual temperature (MAT).

The SMPDSv1 data-set was developed as an environmental calibration data-set to provide training data for palaeoclimate reconstructions (Harrison, 2019a). SMPDSv1 contains the relative abundancies of the 247 most important pollen taxa in 6458 terrestrial samples from Europe, northern Africa, the Middle East, and Eurasia, compiled from multiple different published sources. We use it to reconstruct mean temperature of the coldest month (MTCO).

Deleted:
Deleted: 2019

2.2.2. Core data-sets

We apply the SWAP training set to the RLGH and RLGH3 core data-sets. RLGH is a fossil diatom data-set from The Round Loch of Glenhead, Scotland, taken to explore anthropogenic acidification (Allott et al., 1992). The data-set includes the relative abundances of 41 diatom taxa in 20 samples which span the industrial era. RLGH3 was sampled to explore natural acidification driven by weathering and soil development during the Holocene (Jones et al., 1989). This data-set includes abundances for 225 diatom taxa in 101 samples.

We apply the NIMBIOS training set to the Consuelo and Llaviucu core data-sets. The core from Lake Consuelo, Bolivia, is an 8.8 m sediment sequence, which records the long-term evolution of cloud forest in response to environmental changes over the last 46,300 years (Urrego et al., 2010). Lake Llaviucu is a temperature-sensitive lake in the Ecuadorian Andes (Steinitz-Kannan et al., 1983; Colinvaux et al., 1988). It lies behind a moraine in the system dated by Clapperton (1987) within the last glaciation (35,000 yr B.P.). At nearly 37 degrees S latitude, the lake is perched on the eastern face of the Cordillera Occidental and has been lifted 2,200 m since deglaciation. It shows the possibility of significant cooling of tropical latitude rain-forest near San Juan Bosco (Colinvaux et al., 1997).

We apply the SMPDSv1 training set to the Villarquemado core data-set (Harrison 2019, Wei et al 2021a), a pollen record from the western Mediterranean Basin spanning the interval from the last part of MIS-6 to the late Holocene. The fossil pollen data were assigned to the subset of pollen taxa recognised in the modern SMPDSv1 data-set. There are 104 taxa represented in the final taxon list based on the 361 core samples.

2.3. Model parameters, performance, and validation metrics

2.3.1. Model parameters

We build the GloVe model using the PyTorch deep learning frame (Paszke et al., 2019), which provides a set of tools and interfaces to implement, train, and deploy deep-learning models. In embedding training, we set the number of epochs (training loops) to 1,000 and the number of embedding dimensions to 256. For the first layer, we build an ensemble of 1,000 decision trees number with parallel computing. MEMLM has an external interface so that these parameters can be easily changed for any third-party application.

We originally developed the GloVe analysis using the pre-packaged software 'glove-python' [https://github.com/maciejkula/glove-python] but subsequently re-wrote the GloVe algorithm from first principles. Cross-validation and down-core reconstructions from the two algorithms were not materially different and so the statistical significance testing, which is highly expensive computationally, requiring one month of parallel computing, was not repeated.

2.3.2. The prediction importance indicator for taxon weighting

The MEMLM models are ensembles based on the results of multiple decision trees. Each time a decision tree forks, the algorithm explores different ways to integrate each taxon's abundance to increase predictive power. The algorithm works through an internal cross-validation analysis to determine whether each predictor reduces the prediction errors in each decision tree, and then summarises the results across all decision trees. The approach ascribes an importance index to each taxon which is normalised to a total of 1 across all taxa and provides a measure of that taxon's predictive power. The ten most important taxa for each of the three machine-learning models are listed in Table A3. These are used in the inference of taxon importance for climate reconstruction.

Deleted: ¶
Deleted: the glacial age.
Deleted: recognized
Deleted: Performance
Deleted: GLOVE
Deleted: under
Deleted: for efficient matrix computation and error gradient feedback …
Deleted:).
Deleted: 1000
Deleted: 1000
Deleted:
Deleted: note that we
Deleted: GLOVE
Deleted: we
Deleted: GLOVE
Deleted: will explore how
Deleted: values
Deleted: have more
Deleted: summarizes
Deleted: upstream model
Deleted: detailed
Deleted: Tables A2

2.3.3. Uncertainty quantification

Uncertainty quantification is provided for all machine-learning reconstructions using IBM's UQ360 package. We apply the Infinitesimal Jackknife, which performs a first-order Taylor series expansion around the maximum likelihood estimate to provide 25% and 75% confidence intervals of the prediction (IBM, 2024)

2.3.4. Cross-validation

The predictive powers of the MEMLM variants are compared with classical WA models (ter Braak and Barendregt, 1986) and WA-PLS (ter Braak and Juggins, 1993). We take RMSEP, regression slope, and R^2 score as performance evaluation indicators, using the scikit-learn package (Pedregosa et al., 2011). We use five-fold cross-validation. We perform each cross-validation five times with random shuffling allowing us to provide mean estimates for all validation metrics along with their standard deviations, which we provide for RMSEP. We note that spatial correlation and pseudo-replication within a training set can lead to overstated cross-validated performance statistics. These problems can be minimised by, for instance, removing sites that are geographically and climatically close (Liu et al., 2020). However, we include all training-set sites in cross-validation, noting that our objective is to compare the relative performances of different approaches applied to the same training sets. For evaluation of the classical models we use the rioja package in R (Juggins, 2017) with default settings. As WA-PLS performance is sensitive to the number of components; we accept a higher PLS component only if it exhibits a 5% improvement in RMSEP on the previous component (Birks, 1998) and we present results for the higher component.

2.3.5. Statistical significance of reconstructions

While cross-validation is a useful measure of predictive power which implicitly guards against over-fitting (Yates at al., 2023), it is likely to over-estimate predictive power in practice as fossil assemblages may lie outside the high dimensional space of the modern training assemblages, for instance by lacking close modern analogues. Telford and Birks (2011) developed an easily applied method for testing the robustness of a reconstruction of a specific site. The approach is to create an ensemble of transfer functions using the same biological assemblage as the training set, but with randomised values of the environmental variable. If the reconstructed variable is found to explain more of the variance than 95% of the random reconstructions, then the reconstruction is deemed to be statistically significant. We apply this approach with the palaeoSig package in R (Telford and Trachsel, 2015) to all core reconstructions as an indicator of their robustness.

2.4. Computing hardware

In this study, the computing CPU is Intel Core i7-4710MQ; the model is supported by the scikit-learn package (Pedregosa et al., 2011), a powerful machine learning Python package which incorporates the most widely used machine-learning algorithms and related data processing and validation functions. MEMLM supports parallel computing: with more CPU cores, the

Deleted: 2012

Deleted:

Deleted: this study

Deleted: that

Deleted: 4

Deleted: ,

Deleted: tests a model for

Deleted: .

Deleted: Birks

Deleted: 2012).

computing time will decrease significantly. The computational time taken for five-fold cross-validation of the MEMLMc model is 138 seconds (SWAP), 406 seconds (NIMBIOS), and 2834 seconds (SMPDsV1).

3 RESULTS

3.1. Cross-validation

Table 1 compares the cross-validated RMSEP for the three training sets and the six reconstruction approaches (see Figure A1 for regression visualization of predicted values against observed values). Regression slope and R^2 score are also provided. All validation data are the means of five separate cross-validation exercises, which are also used to provide a percentage error estimate for RMSEP (in brackets). WA-PLS is found to be the best performing classical approach in all three training sets as evaluated by RMSEP, but in each case it is outperformed by MEMLM, which reduces RMSEP by 6% (SWAP, 167 training samples, 277 taxa), 22% (NIMBIOS, 636 training samples, 533 taxa), and 50% (SMPDSv1, 6548 samples, 257 taxa). The benefits of machine-learning approaches clearly increase with increasing training-set size.

MEMLMe is trained only on embedded assemblage data from GloVe. The approach does not work well for the SWAP training set, but it significantly improves upon WA approaches when using the larger NIMBIOS and SMPDVs1 training sets, suggesting that when the training set is large enough, embedding is able to extract most of the predictive power of the assemblages. However, MEMLMe is consistently the worst performing MEMLM variant (albeit generally better than the WA approaches), and so we do not use it in the reconstructions.

We performed additional cross-validation tests on MEMLMe to confirm that the embedding approach can encode useful information, noting that with an embedding dimension of 256 (comparable to the number of taxa in the training sets) we are not applying the approach under significant dimensional reduction. To explore this, we applied a range of embedding dimensions to the MEMLMe model of the richest data-set, being the 533-taxon NIMBIOS data-set (Figure A2a). This sensitivity demonstrates that 30 dimensions are sufficient for MEMLMe to outperform WA-PLS (RMSEP 2.914°C) in this training set. Figure A2b illustrates the learning power of increased training, with RMSEP increasing by around 0.4°C as the number of training epochs is reduced from the 1,000 we used to 40.

MEMLMc uses both the taxon abundance and the embedding matrices. These additional data do not significantly affect the predictive performance relative to MEMLM under cross-validation, suggesting that conventional ensemble machine-learning approaches are sufficient to encode adequately the assemblage information in training sets comprising a few hundred taxa. However, we retain this model for down-core reconstructions to explore whether the addition of embedding information can affect reconstructions in a way that is not captured by RMSEP.

Formatted: Font colour: Black
Formatted: Font colour: Auto
Formatted: Font colour: Black
Deleted: five
Deleted: See
Deleted: WA-PLS was
Deleted: was
Deleted: reduced
Deleted:)
Deleted: additional
Deleted: power
Deleted: is evident
Deleted: GLOVE
Deleted: under- performs relative to
Deleted: and MEMLMc,
Deleted: does indeed
Deleted: We
Deleted: progressively increasing
Deleted: dimension applied
Deleted: an
Deleted: MAT using
Deleted: A1b
Deleted: only about
Deleted: -
Deleted: required
Deleted:), so that that dimension reduction by more than an order of magnitude retains sufficient information to build a useful model. Increasing the embedding dimension towards 256 unsurprisingly progressively improves RMSEP further by encoding additional assemblage information.
Deleted: decreasing
Deleted: increased
Deleted: to 1000
Deleted: -
Deleted:
Deleted:
Formatted: Font colour: Black
Formatted: Centred, Indent: First line: 0.74 cm, Space Before: 0.5 line, After: 0.5 line

		MEMLM	MEMLMe	MEMLMc	WA-Inv	WA-Cla	WA-PLS(best)
RMSEP							
SWAP	pH	**0.290 (3.7%)**	0.331 (3.1%)	0.296 (2.8%)	0.308 (1.1%)	0.317 (1.0%)	0.308 (1.1%)
NIMBIOS	MAT/°C	2.254 (1.6%)	2.221 (1.2%)	**2.094 (1.4%)**	3.176 (0.5%)	3.587 (0.6%)	2.923 (0.6%)
SMPDSv1	MTCO/°C	**2.353 (0.5%)**	2.779 (0.9%)	2.478 (0.6%)	5.310 (0.1%)	6.672 (0.1%)	4.979 (0.2%)
Slope							
SWAP	pH	0.984	1.002	0.999	1.029	0.899	1.030
NIMBIOS	MAT/°C	0.996	0.998	**0.999**	1.005	0.750	0.996
SMPDSv1	MTCO/ °C	0.997	0.997	0.997	1.000	0.629	0.996
R^2 score							
SWAP	pH	**0.858**	0.815	0.852	0.840	0.831	0.840
NIMBIOS	MAT/ °C	0.856	0.860	**0.876**	0.714	0.635	0.758
SMPDSv1	MTCO/°C	**0.926**	0.897	0.918	0.624	0.407	0.670

MAT mean annual temperature; MTCO mean temperature of the coldest month

Table 1. Cross-validated root mean square error of prediction (RMSEP), regression slope, and R^2 score for the three training sets. All data are the means of five cross-validation exercises, which are also used to provide uncertainty estimates for RMSEP (percentage error for RMSEP in brackets). MEMLM uses the abundance matrix. MEMLMe uses the assemblage embedding matrix. MEMLMc uses the spliced abundance and embedding matrices. WA-Cla is weighted averaging with a classical deshrinking regression, WA-Inv is weighted averaging with an inverse deshrinking regession (Birks et al., 1990). WA-PLS is the 'best' model (see section 2.2.3), see Table A4 for other components. Bold highlights the model with the lowest RMSEP or highest R^2 score.

3.2. Environmental reconstructions and comparisons

For each core we compare the reconstructions from the models with lowest RMSEP, being the MEMLM and MEMLMc machine-learning approaches and the best classical approach (section 2.3.3), which is WA-PLS using one component for SWAP and WA-PLS using two components for NIMBIOS and SMPDSV1. In the Appendix, Figures A3 to A7 illustrate scatterplot matrices of all six reconstruction approaches, and Figures A8 to A12 compare reconstructions for all six models through time. In each reconstruction we additionally provide the statistical significance test results (Telford and Birks, 2011).

Deleted: Cla
Formatted ... [5]
Deleted: Inv
Formatted ... [6]
Deleted:
Formatted ... [7]
Deleted: ¶
Formatted ... [8]
Formatted ... [2]
Formatted ... [3]
Formatted ... [4]
Formatted ... [9]
Formatted ... [10]
Formatted Table ... [11]
Formatted ... [12]
Formatted ... [13]
Formatted ... [14]
Formatted ... [15]
Formatted ... [16]
Formatted ... [17]
Formatted ... [18]
Formatted ... [19]
Formatted ... [20]
Deleted: 289
Formatted ... [21]
Deleted: 376
Formatted ... [22]
Deleted: 294
Deleted: 299
Formatted ... [23]
Formatted ... [26]
Deleted: 307
Formatted ... [24]
Deleted: 313
Formatted ... [25]
Deleted: 203
Deleted: 193
Deleted: 092
Deleted: 914
Formatted ... [27]
Formatted ... [29]
Formatted ... [30]
Formatted ... [31]
Formatted ... [32]
Formatted ... [33]
Formatted ... [36]
Formatted ... [28]
Deleted: 194
Deleted: 577
Formatted ... [34]
Formatted ... [35]
Deleted: 360
Deleted: 827
Deleted: 449

A reconstruction is considered significant when that reconstruction explains more of the variance than 95% of 1,000 randomised reconstructions, based on the same training assemblage but with randomised environmental values.

Deleted: 1000

Deleted: which apply

Deleted: randomized

Deleted: characteristics

3.2.1. pH reconstructions from RLGH using the SWAP training set

MEMLM and WA-PLS1 show similar trends of acidification, with pH declining from around 5.2 at about 1870 to around 4.8 at about 1980 (see Figure 2). MEMLMc shows a similar trend but with reduced acidification relative to the other approaches. All three reconstructions are statistically significant, and with high explained variance, though WA-PLS1 explains more variance (58%) than MEMLM (46%) or MEMLMc (52%.). The variance explained by the first principal component of the fossil core assemblages is 62%, indicating that the reconstructed pH explains most of the dominant part of the variance in the fossil diatom assemblages.

Deleted: .

Deleted: understates the degree of

Deleted: (Figure 2).

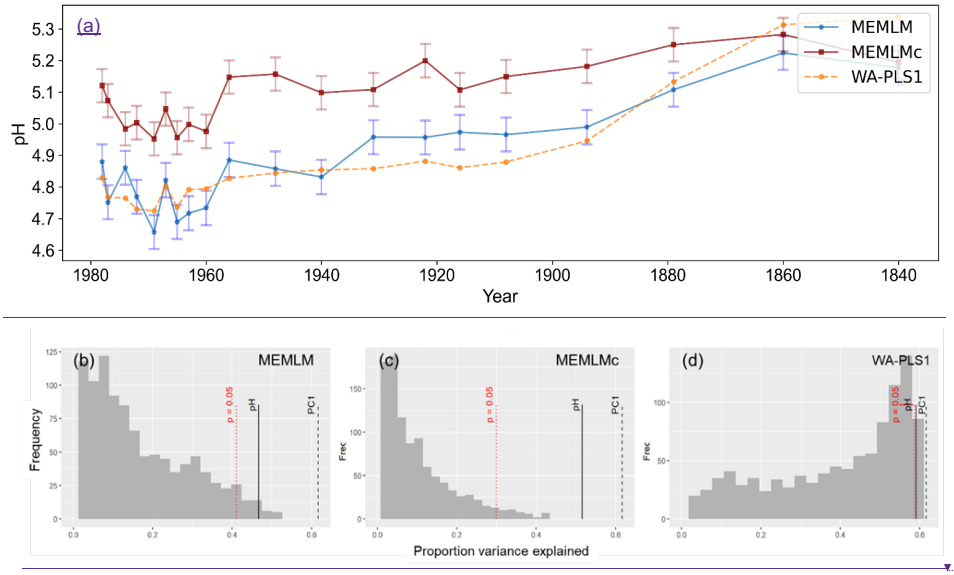

Figure 2: a) pH reconstruction for the RLGH core. b, c & d) statistical significance of MEMLM, MEMLMc, and WA-PLS1 reconstructions, respectively. MEMLM uncertainties are calculated using IBM UQ360 (section 2.3.3). These compare with cross-validated RMSEP errors of 0.292 (MEMLM), 0.294 (MEMLMc), and 0.308 (WA-PLS1) pH units.

3.2.2. pH reconstruction from RLGH3 using SWAP

All three methods provide reconstructions that show similar trends of lake-water pH, with gradual acidification in the early record from around 5.6 to 5.2 pH, attributed to the development of organic soils (Jones et al., 1989) and then a rapid post-

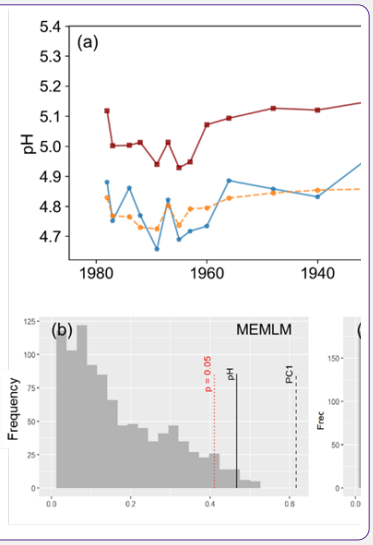

Deleted:

industrial acidification from around 5.2. to 4.8 pH. The three reconstructions also exhibit similar variability, previously attributed to loss of tree cover and peat erosion (Jones et al., 1989), further suggesting reconstruction robustness. Moreover, all three reconstructions are statistically significant, explaining between 23% and 27% of the core variance, which compares to 32% variance explained by the first principal component of the fossil assemblages (Figure 3).

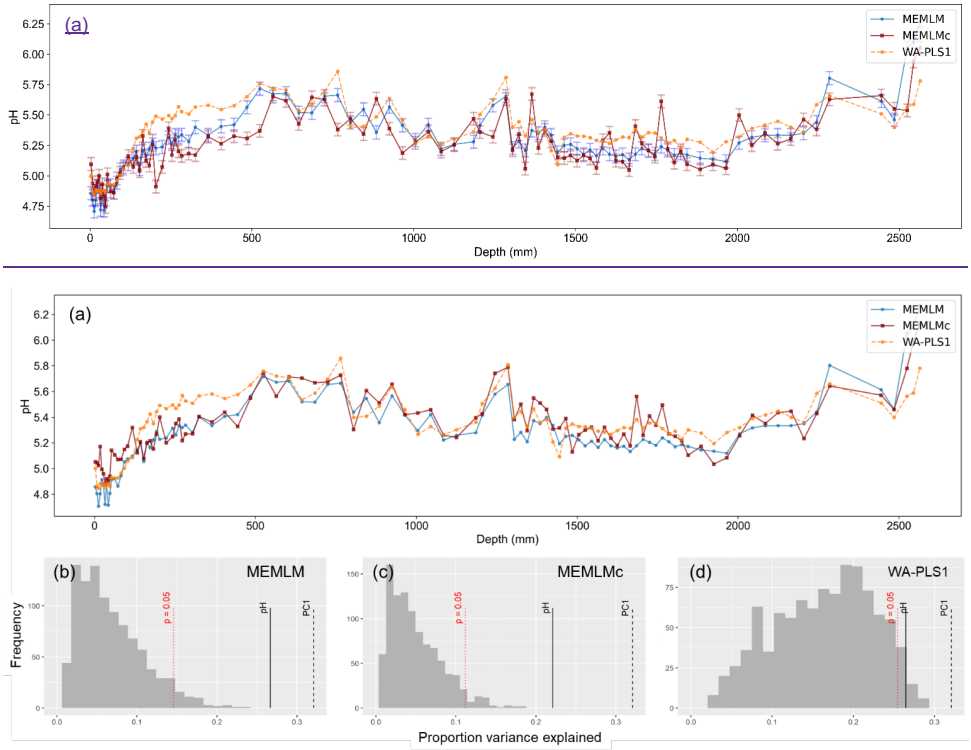

Figure 3: a) pH reconstruction for the RLGH3 core. b, c & d) statistical significance of MEMLM, MEMLMc, and WA-PLS1 reconstructions, respectively. MEMLM uncertainties are calculated using IBM UQ360 (section 2.3.3). These compare with cross-validated RMSEP errors of 0.292 (MEMLM), 0.294 (MEMLMc), and 0.308 (WA-PLS1) pH units.

Deleted:

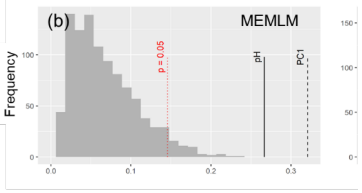

3.2.3. MAT reconstruction from Consuelo using the NIMBIOS training set

All three methods display similar trends, most notably reconstructing about a 4°C warming from the Last Glacial Maximum at 21,000 BP to the start of the Holocene at 11,000 BP. The MEMLM approaches are more variable in general, although variability is largely synchronous between the three reconstruction approaches and may be associated with Dansgaard-

Oeschger (D/O) events (Bond et al., 1993; Blunier and Brook, 2001). At 8000 BP, WA-PLS2 displays a 10°C cooling excursion which is not apparent in the MEMLM reconstructions. Although a cooling event at 8.2ka is well known, the cooling reconstructed by WA-PLS2 cooling seems excessive. All three methods are statistically significant and explain core assemblage variance of between 27% and 29%, compared to 32% explained by the first principal component (Figure 4).

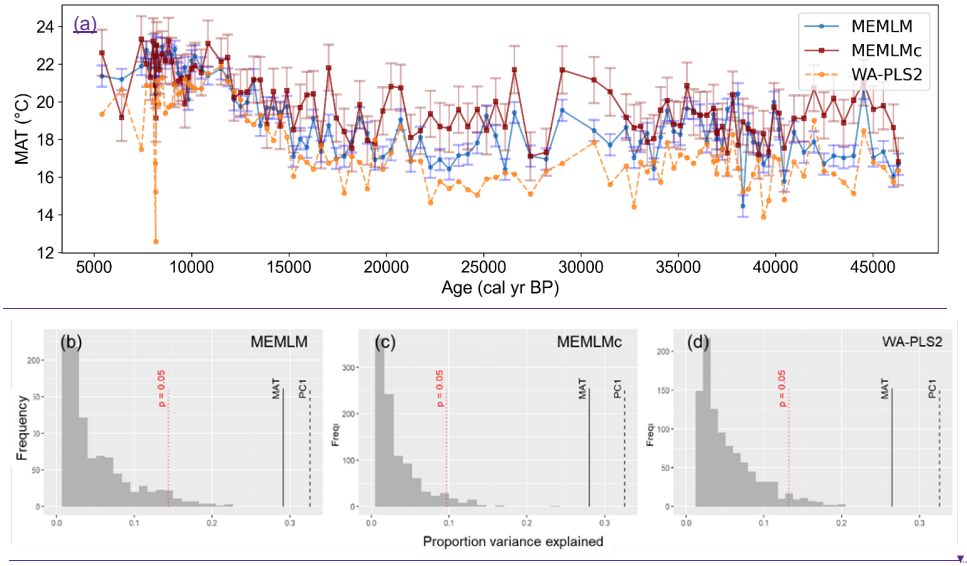

Figure 4: a) MAT reconstruction for the Consuelo core. b, c & d) statistical significance of MEMLM, MEMLMc, and WA.PLS2 reconstructions, respectively. MEMLM uncertainties are calculated using IBM UQ360 (section 2.3.3). These compare with cross-validated RMSEP errors of 2.254 (MEMLM), 2.094 (MEMLMc), and 4.979 (WA-PLS2) °C.

3.2.4. MAT reconstruction from Llaviucu by the NIMBIOS training set

All three methods display similar overall trends with mid-Holocene warming, but each display different centennial variability, which for the MEMLMc reconstruction is clearly unrealistic for the Holocene, with temperature excursions as large as 8°C. Neither of the MEMLM approaches are statistically significant at the 95% confidence level, so neither can be accepted as robust. The WA-PLS2 reconstruction is statistically significant, although it only explains 13% of the core assemblage variance compared to the 28% explained by the first principal component of the core data (Figure 5).

Deleted: .

Deleted: &

Deleted: is

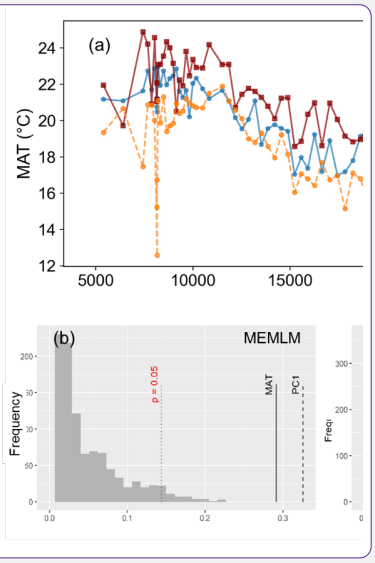

Deleted:

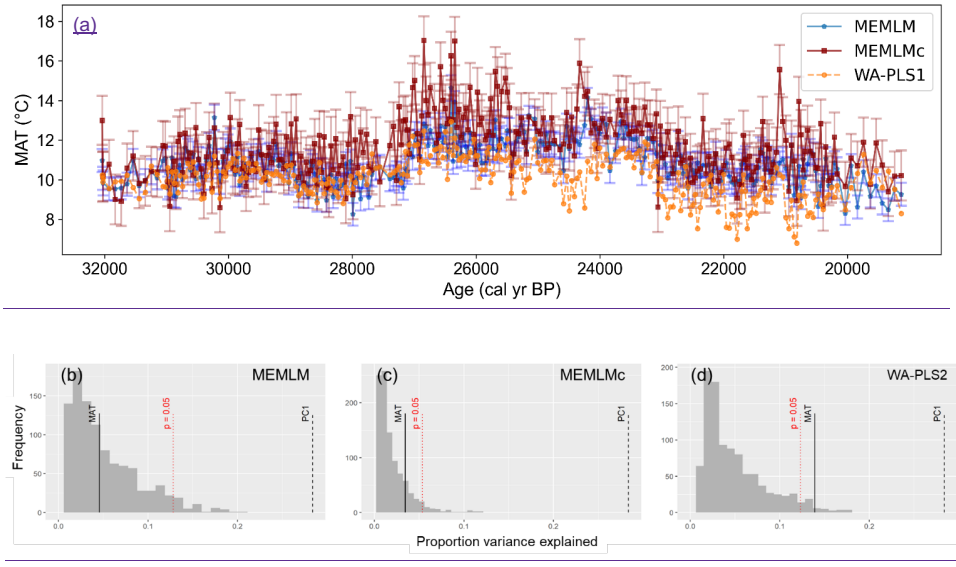

Figure 5: a) MAT reconstruction for the Llaviucu core. b, c & d) statistical significance of MEMLM, MEMLMc, and WA-PLS2 reconstructions, respectively. MEMLM uncertainties are calculated using IBM UQ360 (section 2.3.3). These compare with cross-validated RMSEP errors of 2.254 (MEMLM), 2.094 (MEMLMc), and 4.979 (WA-PLS2) °C.

3.2.6. Reconstruction for core Villarquemado using the SMPDSV1 training set

All three approaches generate noisy reconstructions with high variability that is incoherent. It is difficult to discern any meaningful trends. None of the reconstructions, including WA-PLS2, are statistically significant. The low (17%) variance associated with the first principal component suggests that the fossil assemblages are responding to multiple environmental factors with responses that are too complex to be captured by a single explanatory environmental variable (Figure 6).

Deleted:

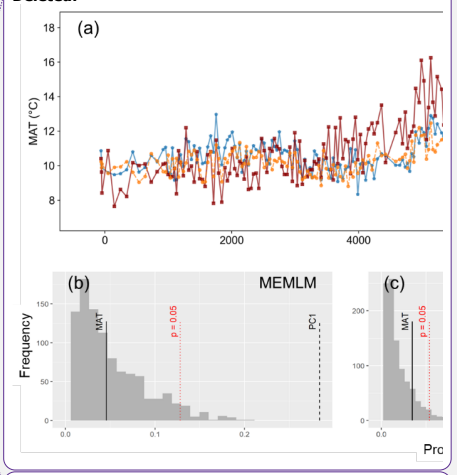

Deleted: inconsistent

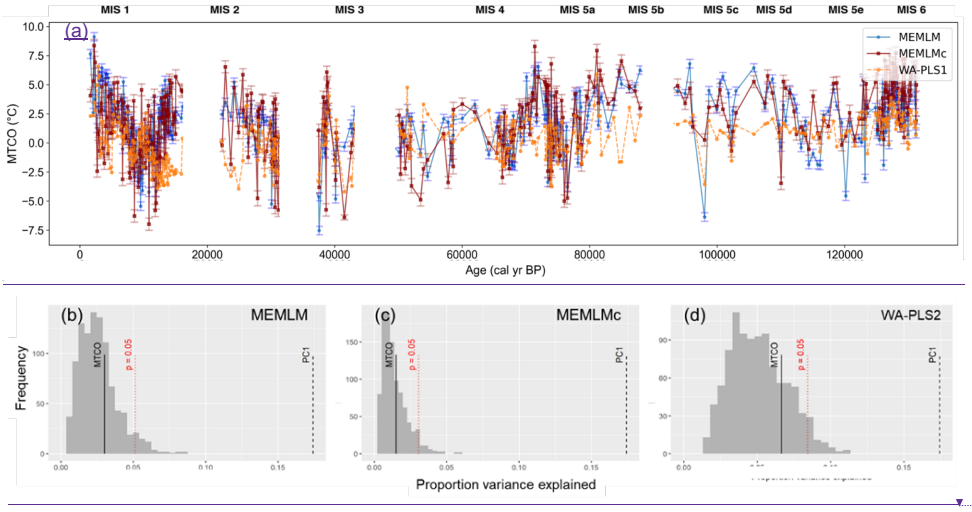

Figure 6: a) MTCO reconstruction for the Villarquemado core. b, c & d) statistical significance of MEMLM, MEMLMc, and WA-PLS2 reconstructions, respectively. MEMLM uncertainties are calculated using IBM UQ360 (section 2.3.3). These compare with cross-validated RMSEP errors of 2.353 (MEMLM), 2.434 (MEMLMc), and 2.923 (WA-PLS2) °C.

4 Discussion and conclusions

We have developed three variants of a multi-model ensemble machine-learning algorithm, MEMLM. These each train three separate ensemble machine-learning algorithms (random forests, extremely random trees and lightGBM) and combine them into a consensus reconstruction using multiple regression. The three approaches only differ in their input data. The simpler MEMLM takes only taxon abundance data. MEMLMe, built only upon the GloVe embedding matrix, does not perform as well as MEMLM. However, MEMLMe was found to be a useful reconstruction model, at least when applied to the larger NIMBIOS and SMPDSV1 training sets, and the embedding usefully summarises taxon assemblages with fewer than 50 dimensions. Our motivation for retaining 256 embedding dimensions in MEMLMe is that the focus of GloVe is on extracting semantic meaning. In linguistics, typically 200 dimensions of meaning are needed to fully encode a language. While we have shown that far fewer dimensions are sufficient to build a good reconstruction model, demonstrating the explanatory power of the most important embedding dimensions, there are progressive improvements in performance as dimensional size increases. This demonstrates that less important dimensions can provide useful explanatory information, and potentially additional understanding and interpretability.

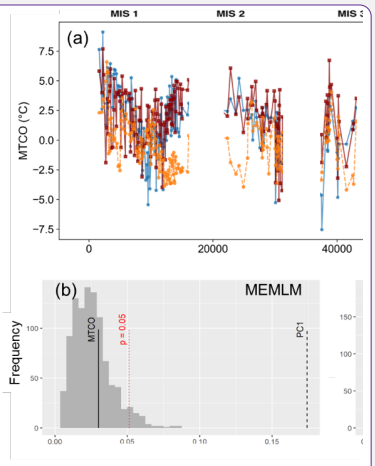

Deleted:
Formatted: Font colour: Black
Formatted: Font colour: Auto
Formatted: Font colour: Black
Deleted:
Deleted:
Deleted: a weak learner approach based on
Deleted: GLOVE
Deleted: was able to
Deleted: summarise

The additional complexity of MEMLMc, which uses both taxon count and embedding, did not significantly affect the predictive performance relative to MEMLM under cross-validation, suggesting that conventional ensemble machine learning approaches are sufficient to encode adequately ecological information in the relatively small data-sets used in these palaeoclimate reconstructions. We note that the real power of embedding (dimension reduction) approaches is likely to be in their applications to much larger data-sets, when ecological relationships between 10,000s of taxa and their environment are being considered.

We have focussed only on a comparison with weighted averaging approaches, which are the most widely used reconstruction technique, being simple to apply, well understood, and straightforward to interpret. The MEMLM approaches are found to perform better than classical weighted averaging approaches under cross-validation. In the case of the smallest SWAP data-set the advantages are modest, but in the largest SMPDSV1 data-set RMSEP errors are reduced by a factor of two relative to the best performing classical WA approach. These improvements in performance clearly validate the potential benefits of strong data-mining abilities of machine learning, suggesting these techniques have the potential to improve upon classical reconstruction approaches.

When applied to core reconstructions, MEMLM approaches generate considerably more variability than the WA-PLS reconstructions. While some elements of this additional variability might be realistic, especially considering that WA-PLS approaches are known to bias reconstructions towards the centre of their training data (Liu et al., 2020), the variability is not always coherent between different reconstruction approaches and the magnitude of MEMLM variability is in some cases implausibly high, for example by suggesting Holocene variability of up to 8°C in the Ecuadorian Llaviucu core.

We performed significance testing on all core reconstructions and find that five of the fifteen reconstructions are not statistically significant and therefore are not considered robust. encode Both MEMLM and MEMLMc approaches fail on the Llavuicu core, confirming our suspicion that the unrealistic variability is an artefact even though the overall trends of the reconstruction are consistent with the robust WA-PLS2 reconstruction. All three approaches fail the statistical robustness test at Villarquemado, which is sensitive to multiple environmental factors and has responses which appear too complex to be captured by a single explanatory variable.

The shapes of the histograms of the proportion of variance explained in the RLGH and RLGH3 pH reconstructions based on diatom data and randomised modern SWAP training pH values in the significance testing are very different for WA-PLS1 and for MEMLM and MEMLMc (Figs. 2, 3). Such differences contrast with the more consistent histogram shape for the significance-test results for the other sequences where the reconstructions are based on pollen data (Figs. 4–6). Machine-learning approaches generally fail badly when trained with randomised environmental data as the histograms are left-skewed and explain little down-core variance (Figs. 2–6). In contrast, the WA-PLS1 pH reconstructions (Figs. 2, 3) based on diatom data explain a substantial amount of the down-core variance even when the modern pH data are randomised (Figs. 2, 3). This may result from the short and dominant environmental gradient in the SWAP diatom–pH training data and the high inherent correlation and dominance of a relatively few abundant taxa within the modern and fossil diatom data. The pollen training data, however, used for the MAT or MTCO reconstructions of the other sequences (Figs. 4–6) are large (638 and 6,458

Deleted:
Deleted: in ecology
Deleted: 000's
Deleted: were both
Deleted:
Deleted: were
Deleted: were
Deleted:
Deleted: to create a more complete description of a data-set
Deleted: were found to
Deleted: was
Deleted: found to be
Deleted: was
Deleted: found
Deleted: were
Deleted: should
Deleted: be
Deleted: failed
Deleted: was
Deleted: were
Deleted: failed

samples) and hence cover longer and more complex environmental gradients than the pH training data (167 samples). It is also likely that the pollen data, both modern and fossil, are influenced by multiple environmental factors, not only MAT or MTCO. In summary, while MEMLM can generate useful reconstructions, it should always be used in conjunction with statistical significance testing to confirm that the reconstructions are robust and potentially realistic and reliable. The additional complexities of incorporating embedding information in MEMLMc does not reduce RMSEP or spurious variability and neither does it improve statistical significance. However, MEMLMe demonstrates that embedding is useful as it can summarise ecological assemblages using significantly fewer dimensions. Its benefits may be clearer in applications with much larger data-sets and in applications beyond palaeoenvironmental reconstructions. The poor performance of MEMLM in some reconstructions may be due to extrapolation due to poor or no analogue fossil assemblages. All models are applied under the same extrapolation. The WA-PLS2 reconstructions exhibit higher statistical significance than MEMLM, although WA-PLS2 also fails to generate robust reconstructions at Villarquemado. We infer that that the use of simpler WA models, which include a major biological assumption (unimodal environmental response) can be more powerful than the use of brute-force learning, despite reductions in RMSEP. We reiterate our recommendation that all reconstructions using any approach, should be accompanied with statistical significance testing. Seemingly useful models may fail when applied under extrapolation or when the assemblage variance is only weakly dependent on the reconstructed environmental variable.

Deleted: ensure
Deleted: providing assemblage
Deleted: to
Deleted: did
Deleted: nor did
Deleted: demonstrated
Deleted: felt more clearly
Deleted: to
Deleted: Even though all
Deleted: were
Deleted: , the
Deleted: were found to be more reliable
Deleted: failed

Acknowledgements

PS was funded by a PhD scholarship from the China Scholarship Council (CSC, no. 202104910033). HJBB's participation has been possible thanks to the European Research Council under the European Union's Horizon 2020 Research and Innovation Programme grant agreement 74143 to the project 'HOPE: Humans on Planet Earth - long-term impacts on biosphere dynamics' awarded to HJBB. We thank Mark Bush and Alex Correa-Metrio for generously providing the NIMBIOS modern pollen data and Llaviucu fossil pollen data and Graciela Gil Romera for generously providing the SMPDS v1 modern pollen data and Villarquemado fossil pollen data. We are grateful to Cajo ter Braak and Andrew Parnell for valuable comments that improved the manuscript. HJBB thanks Cathy Jenks for her invaluable help.

Formatted: Font colour: Black
Formatted: Font colour: Auto
Formatted: Font colour: Black
Deleted: Prof
Deleted: & Dr
Deleted: Prof
Formatted: Font colour: Auto
Deleted: the public

Data availability

All data-sets can be found in the cited data-sets and articles in references, except the RLGH3 and Llaviucu core, which were made available to us by Mark Bush on request.

Formatted: Font colour: Auto
Deleted: datasets
Deleted: datasets
Formatted: Font colour: Auto
Deleted: are
Deleted: from the authors
Formatted: Font colour: Auto
Formatted: Font colour: Auto

Code availability

All codes are available in github. WA and WA-PLS use the *rioja* package (https://github.com/nsj3/rioja). Telford and Birks (2011) statistical significance uses *randomTF* in the *palaeoSig* package (https://github.com/richardjtelford/palaeoSig). MEMLM can be found at https://github.com/Schimasuperbra/MEMLM

Competing interests

The authors declare that they have no conflict of interest.

Author contributions

PS conceptualised the application of GloVe to ecological assemblages. PS, PBH and HJBB conceptualised the experimental design. PS developed the MEMLM model and performed all analyses and graphical visualisations. HJBB contributed assemblage data. PS and PBH wrote the manuscript with reviewing and editing by HJBB.

Formatted: Font colour: Blue
Formatted: Font colour: Blue
Formatted: Font colour: Blue
Formatted: Font colour: Blue
Formatted: Font colour: Blue
Formatted: Font colour: Blue
Deleted: contribution
Formatted: Font colour: Auto
Formatted: Font colour: Auto
Deleted: GLOVE
Deleted: analysis
Deleted: visualisation.

Appendices A

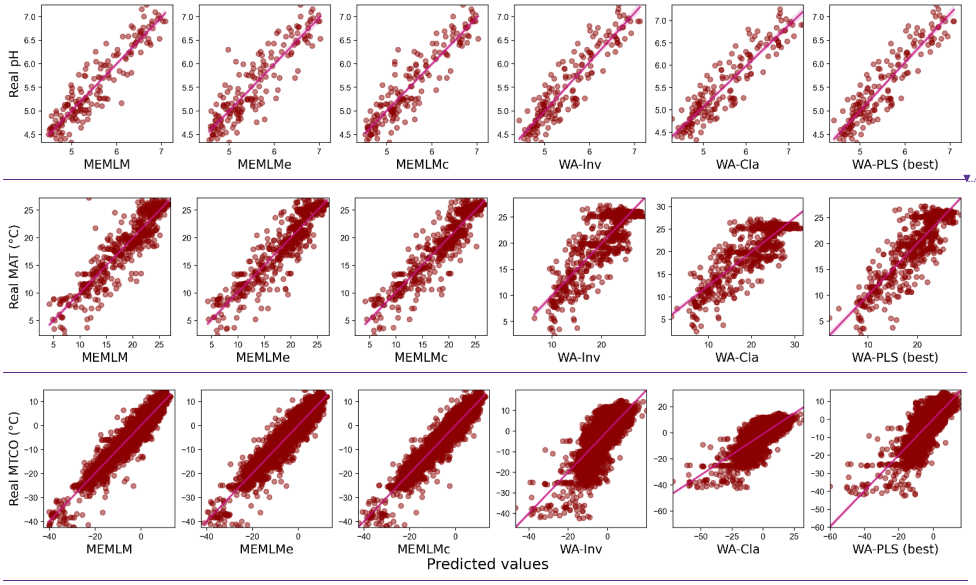

Figure A1: Scatterplots of predicted values against observed values in three training sets. MEMLM uses the abundance matrix. MEMLMe uses the assemblage embedding matrix. MEMLMc uses the abundance and the assemblage embedding matrices. Component number of WA-PLS was selected for each training set as the lowest component that showed a 5% improvement over the previous component (Table A4). WA-Cla is weighted averaging with a classical deshrinking regression, WA-Inv is weighted averaging with an inverse deshrinking regression (Birks et al. 1990). The number of WA-PLS components is selected based on the method described in 2.3.3, see Table S3 for full results.

Formatted: Font colour: Auto

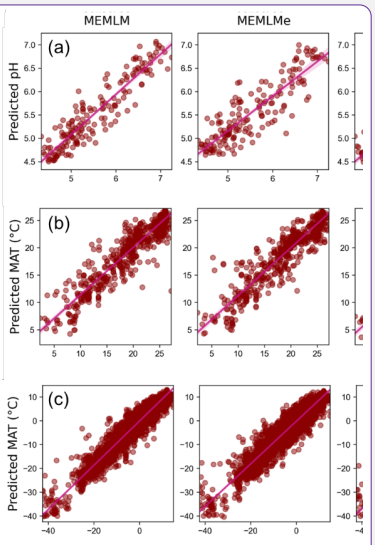

Deleted:

Deleted: Regression visualization

Deleted: A3

Deleted: PLS's

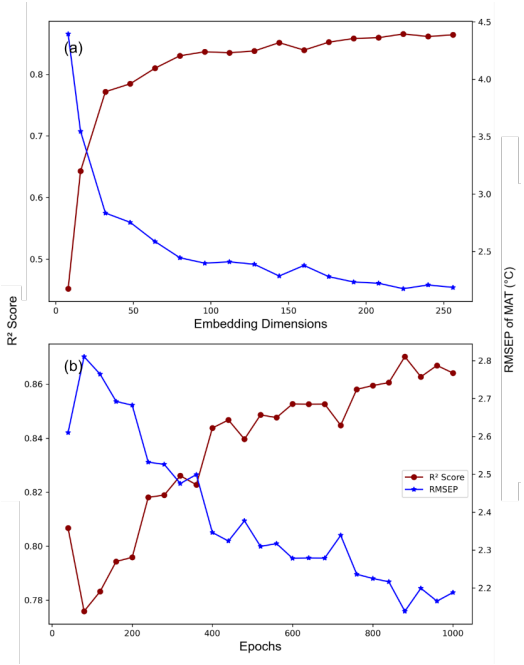

Figure A2: MEMLMe prediction performance under different GloVe hyper-parameter settings. a) Fix epoch = 1,000, set embedding dimensions from 8 to 256; b) Fix embedding dimensions = 256, set epoch from 40 to 1,000. The model is developed from the NIMBIOS set and trained on mean annual temperature (MAT).

Deleted: GLOVE

Deleted: 1000

Deleted: 1000

Deleted: upon

Deleted: .

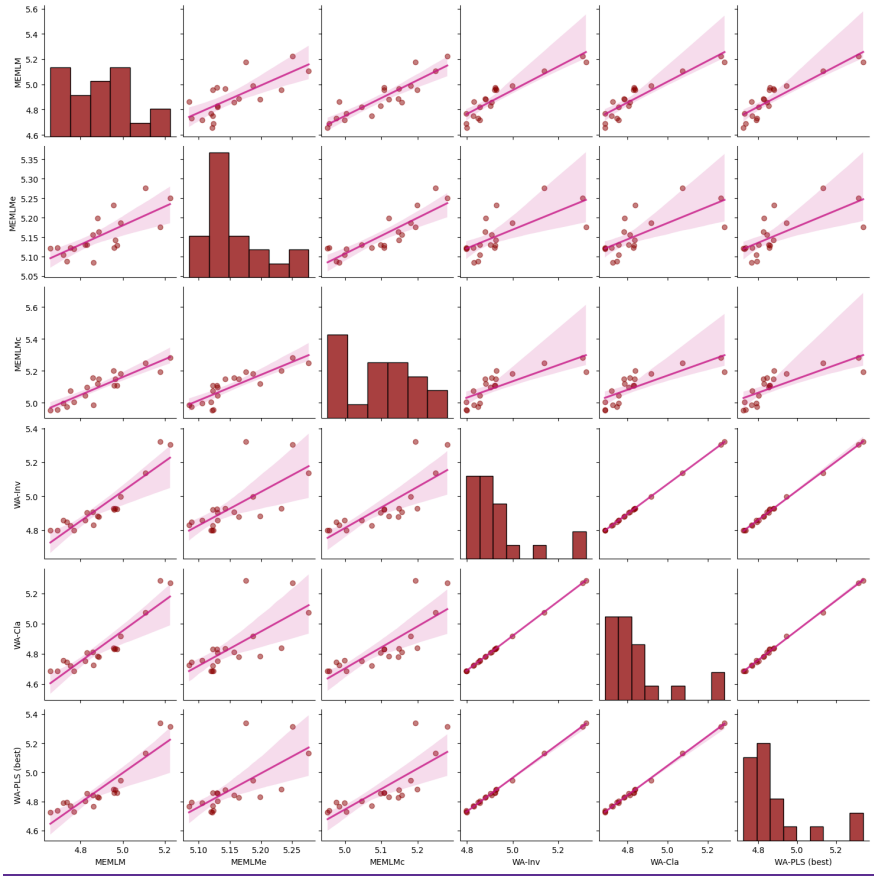

Figure A3: Inter-regression of pH reconstructions for six different models for the Round Loch of Glenhead (RLGH) core.

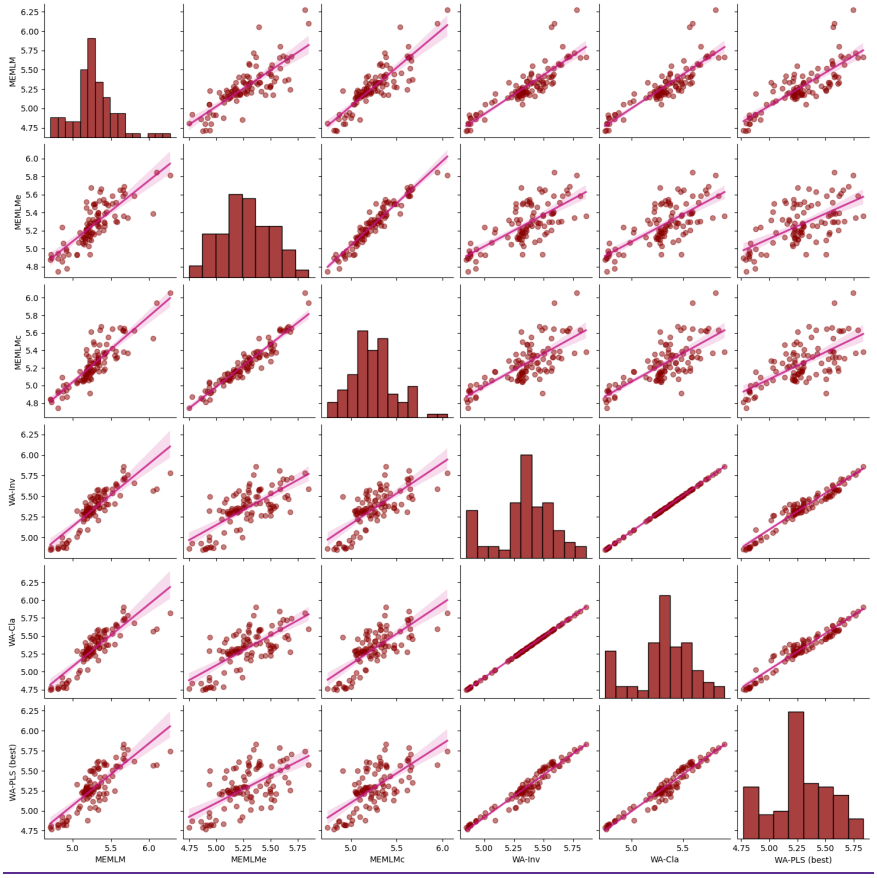

Figure A4: Inter-regression of pH reconstructions for six different models for the Round Loch of Glenhead 3 (RLGH3) core.

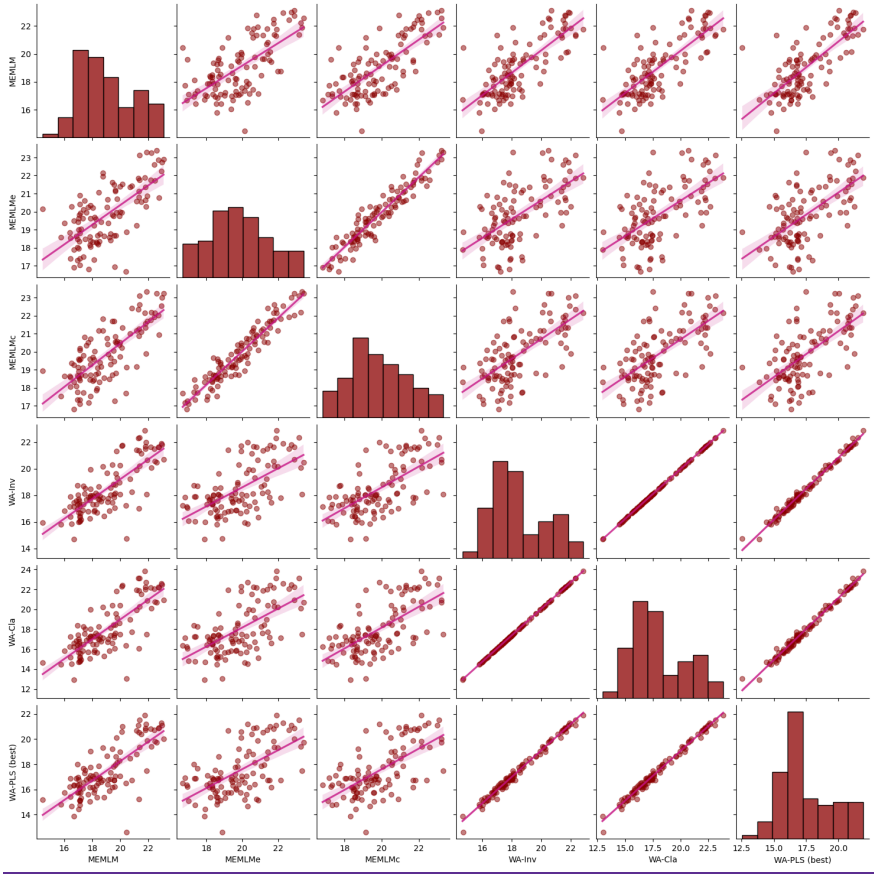

Figure A5: Inter-regression of MAT reconstructions for six different models for the Consuelo core.

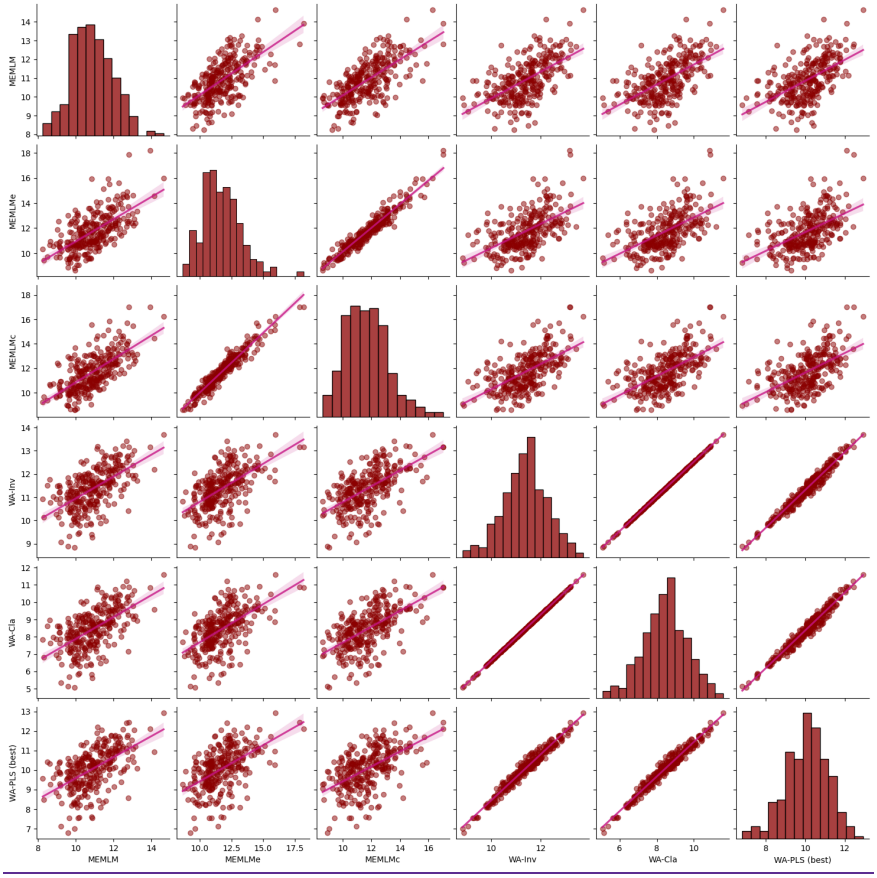

Figure A6: Inter-regression of mean annual temperature (MAT) reconstructions for six different models for the Llaviucu core.

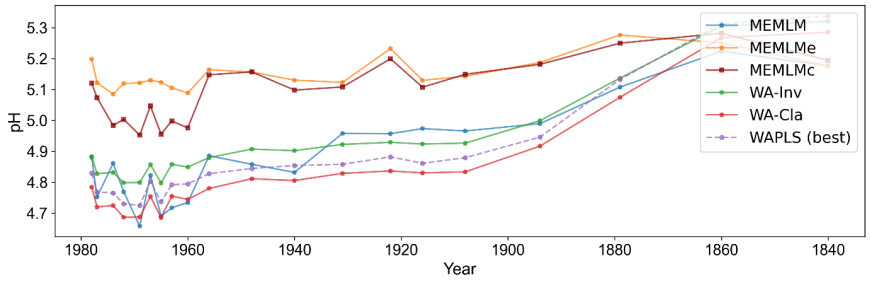

Figure A8: pH reconstructions based on six models for the Round Loch of Glenhead (RLGH) core.

855

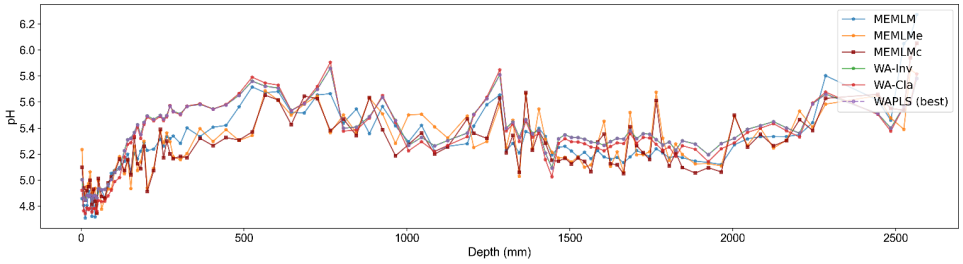

Figure A9: pH reconstruction based on six models for the Round Loch of Glenhead 3 (RLGH3) core.

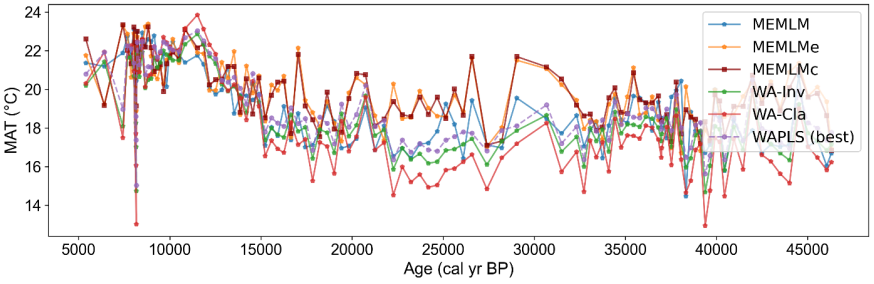

Figure A10: Mean annual temperature (MAT) reconstruction based on six models for the Consuelo core.

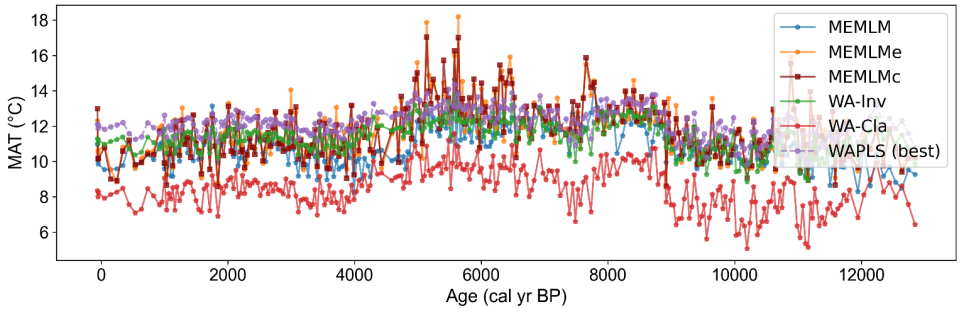

Figure A11: Mean annual temperature (MAT) reconstruction based on six models for the Llaviucu core.

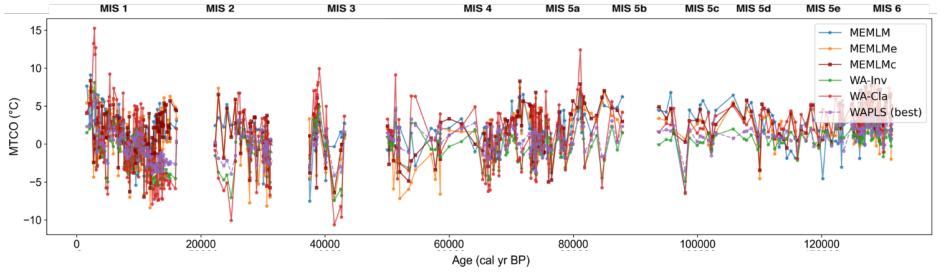

Figure A12: pH reconstruction based on six models for the Villarquemado core.

Table A1: Root mean square error of prediction (RMSEP) and R^2 values (based on cross-validation) of the 18 environment elements prediction of MEMLMc in the NIMBIOS data-set. Mean is average of the prediction of the three downstream models. RF presents the random forest values; ERT presents the extra random tree results. Bold highlights the model with the best prediction performance.

	Elements	RF	ERT	lightGBM	MEMLMc	Mean
RMSEP	Precipitation of the warmest quarter	138.17	131.513	133.124	**125.531**	129.042
	Isothermality	3.065	2.793	3.09	**2.778**	2.838
	Annual precipitation	483.099	442.623	479.217	**430.291**	445.813
	Mean temperature coldest quarter	23.162	21.228	23.061	**21.023**	21.387
	Maximum temperature warmest month	25.104	22.343	24.01	**21.181**	22.421
	Minimum temperature coldest month	26.66	24.15	26.226	**23.734**	24.369
	Mean temperature warmest quarter	22.898	21.435	22.655	**20.727**	21.316
	Precipitation of the coldest quarter	157.458	135.741	151.69	**129.674**	139.075
	Precipitation of the driest month	28.907	25.898	27.892	**23.898**	25.723
	Temperature seasonality	227.1	203.536	221.23	**203.281**	207.248
	Precipitation of the wettest month	64.759	60.669	64.387	**58.822**	60.572
	Temperature annual range	22.179	20.917	22.101	**20.524**	20.83
	Mean temperature wettest quarter	18.312	16.515	18.722	**16.094**	16.865
	Precipitation of the wettest quarter	171.418	161.823	173.802	**157.769**	162.204
	Precipitation seasonality	11.581	10.858	11.506	**10.635**	10.852
	Mean diurnal temperature range	13.139	11.684	12.968	**11.258**	11.855
	Mean temperature driest quarter	23.754	22.225	23.556	**21.989**	22.198
	Precipitation of the driest quarter	96.455	85.831	92.351	**79.657**	85.539
R^2 score	Precipitation of the warmest quarter	0.656	0.688	0.68	**0.716**	0.7
	Isothermality	0.862	0.886	0.86	**0.887**	0.882
	Annual precipitation	0.81	0.841	0.813	**0.85**	0.838
	Mean temperature coldest quarter	0.862	0.884	0.863	**0.886**	0.882
	Maximum temperature warmest month	0.771	0.819	0.79	**0.837**	0.817
	Minimum temperature coldest month	0.887	0.907	0.89	**0.91**	0.905
	Mean temperature warmest quarter	0.85	0.868	0.853	**0.877**	0.87
	Precipitation of the coldest quarter	0.845	0.885	0.856	**0.895**	0.879
	Precipitation of the driest month	0.821	0.857	0.834	**0.878**	0.859
	Temperature seasonality	0.835	**0.868**	0.844	**0.868**	0.863
	Precipitation of the wettest month	0.752	0.782	0.755	**0.795**	0.783
	Temperature annual range	0.848	0.865	0.85	**0.87**	0.866
	Mean temperature wettest quarter	0.822	0.855	0.814	**0.862**	0.849
	Precipitation of the wettest quarter	0.761	0.787	0.755	**0.798**	0.786
	Precipitation seasonality	0.773	0.8	0.776	**0.809**	0.801
	Mean diurnal temperature range	0.803	0.845	0.809	**0.856**	0.84
	Mean temperature driest quarter	0.87	0.887	0.873	**0.889**	0.887
	Precipitation of the driest quarter	0.806	0.846	0.822	**0.868**	0.847

Deleted: ET
Deleted: extended
Deleted: ET
Formatted ... [85]
Formatted ... [86]
Formatted ... [87]
Formatted ... [88]
Formatted ... [89]
Formatted ... [90]
Formatted ... [91]
Formatted ... [92]
Formatted ... [93]
Formatted ... [94]
Formatted ... [95]
Formatted ... [96]
Formatted ... [97]
Formatted ... [98]
Formatted ... [99]
Formatted ... [100]
Formatted ... [101]
Formatted ... [102]
Formatted ... [103]
Formatted ... [104]
Formatted ... [105]
Formatted ... [106]
Formatted ... [107]
Formatted ... [108]
Formatted ... [109]
Formatted ... [110]
Formatted ... [111]
Formatted ... [112]
Formatted ... [113]
Formatted ... [114]
Formatted ... [115]
Formatted ... [116]
Formatted ... [117]
Formatted ... [118]
Formatted ... [119]
Formatted ... [120]
Formatted ... [121]
Formatted ... [122]

Table **A2: Weights of the linear models in MEMLM, MEMLMe, and MEMLMc for the three training sets.**

	MEMLM			MEMLMe			MEMLMc		
Weights	RF	ERT	lightGBM	RF	ERT	lightGBM	RF	ERT	lightGBM
SWAP	-0.238	1.118	0.220	-0.597	1.001	0.619	-0.953	1.062	0.901
NIMBIOS	-0.263	0.934	0.393	-0.793	1.474	0.409	-0.713	1.263	0.533
SMPDSv1	-0.106	0.721	0.431	-0.705	1.180	0.560	-0.340	0.598	0.773

RF – random forest; ERT – extra random tree; lightGBM – a gradient boosting decision tree

Deleted: ¶
Page Break
Formatted: Font: 10 pt, Not Bold
Formatted: Font: 10 pt, Not Bold
Formatted: Font: 9 pt, Bold
Formatted: Font: 10 pt, Not Bold

Table A3: The weights of the 10 most important taxa for the environmental reconstructions in the SWAP, NIMBIOS and SMPDSv1 training sets sorted by the random forests results. Diatom taxon codes follow Stevenson et al. (1991)

	Taxon	RF	ERT	LightGBM
SWAP	EU047A	0.505	0.139	0.033
	AC013A	0.072	0.182	0.028
	EU048A	0.061	0.064	0.02
	TA003A	0.048	0.043	0.017
	PE002A	0.031	0.013	0.027
	CM048A	0.023	0.006	0.029
	BR001A	0.022	0.012	0.032
	TA004A	0.018	0.02	0.017
	NA140A	0.012	0.007	0.01
	CM017A	0.011	0.01	0.019
NIMBIOS	Alnus	0.263	0.096	0.045
	Poaceae	0.146	0.161	0.124
	Plantago	0.118	0.039	0.006
	MoracUrtic	0.105	0.02	0.068
	Bursera	0.049	0.016	0.008
	Myrtaceae	0.024	0.007	0.016
	Ericaceae	0.022	0.042	0.021
	Hedyosmum	0.015	0.03	0.035
	Asteraceae	0.013	0.083	0.056
	Cyperaceae	0.013	0.02	0.068
SMPDSv1	Picea	0.339	0.038	0.029
	Fagus	0.169	0.016	0.012
	Betula Chamaebetula.	0.103	0.22	0.008
	Betula	0.042	0.077	0.041
	Alnus Alnobetula	0.039	0.017	0.007
	Larix	0.03	0.03	0.009
	Quercus deciduous	0.028	0.017	0.03
	Olea	0.027	0.072	0.013
	Oxyria Rumex	0.017	0.009	0.019
	Poaceae	0.014	0.0144	0.028

RF – random forest; ERT – extra random tree; lightGBM – a gradient boosting decision tree

Deleted: top

Deleted: ET

Formatted: Font colour: Auto

Formatted: Font colour: Auto

Formatted Table

Formatted: Font colour: Auto (×31)

Table A4: RMSEP (based on cross-validation) of the first five components (Comp) in weighted-averaging partial least squares (WA-PLS) of the three training sets. Bold highlights the 'best' component, noting that we accept a higher PLS component only if it exhibits a 5% improvement on the previous component (Birks 1998).

Data-set	Feature	WA-PLS Comp1	Comp2	Comp3	Comp4	Comp5
SWAP	pH	**0.308**	0.299	0.313	0.327	0.349
NIMBIOS	MAT	5.310	**4.979**	4.862	4.840	4.863
SMPDSv1	MTCO	3.207	**2.923**	3.022	3.192	3.365

References

Aguirre-Gutiérrez, J., Rifai, S., Shenkin, A., Oliveras, I., Bentley, L. P., Svátek, M., Girardin, C. A. J., Both, S., Riutta, T., Berenguer, E., Kissling, W. D., Bauman, D., Raab, N., Moore, S., Farfan-Rios, W., Figueiredo, A. E. S., Reis, S. M., Ndong, J. E., Ondo, F. E., N'ssi Bengone, N., Mihindou, V., Moraes de Seixas, M. M., Adu-Bredu, S., Abernethy, K., Asner, G. P., Barlow, J., Burslem, D. F. R. P., Coomes, D. A., Cernusak, L. A., Dargie, G. C., Enquist, B. J., Ewers, R. M., Ferreira, J., Jeffery, K. J., Joly, C. A., Lewis, S. L., Marimon-Junior, B. H., Martin, R. E., Morandi, P. S., Phillips, O. L., Quesada, C. A., Salinas, N., Schwantes Marimon, B., Silman, M., Teh, Y. A., White, L. J. T., and Malhi, Y.: Pantropical modelling of canopy functional traits using Sentinel-2 remote sensing data, Remote Sens. Environ., 252, 112122, doi:10.1016/j.rse.2020.112122, 2021.

Allott, T. E. H., Harriman, R., and Battarbee, R. W.: Reversibility of lake acidification at the Round Loch of Glenhead, Galloway, Scotland, Environmental Pollution, 77, 219–225, doi:10.1016/0269-7491(92)90080-T 1992, 1992.

Battarbee, R. W., Monteith, D. T., Juggins, S., Evans, C. D., Jenkins, A., and Simpson, G. L.: Reconstructing pre-acidification pH for an acidified Scottish loch: A comparison of palaeolimnological and modelling approaches, Environ. Pollut., 137, 135–149, doi:10.1016/j.envpol.2004.12.021, 2005.

Birks, H. J. B. ter Braak C. J. F, Line J. M., Juggins S. and Stevenson A. C. Diatoms and pH reconstruction Phil. Trans. R. Soc. Lond. B, 327, 263–278, doi:10.1098/rstb.1990.0062, 1990.

Birks, H. J. B., Numerical tools in palaeolimnology – Progress, potentialities, and problems, J. Paleolimnol., 20, 307–332, doi:10.1023/A:1008038808690, 1998.

Blunier, T. and Brook, E. J.: Timing of millennial-scale climate change in Antarctica and Greenland during the Last Glacial period, Science, 291, 109–112, doi:10.1126/science.291.5501.109, 2001.

Deleted: A3… RMSEP (based on cross-validation) of t … [123]
Deleted: Dataset
Deleted: Comp01
Deleted: Comp02
Deleted: Comp03
Deleted: Comp04
Deleted: Comp05
Deleted: NIMBIOS
Formatted Table … [124]
Deleted: MAT
Deleted: 31.971
Formatted … [125]
Deleted: 29.136
Deleted: 30.224
Deleted: 31.712
Deleted: 33.557
Deleted: SMPDSv1
Moved up [1]: MTCO
Formatted … [126]
Deleted: 304
Formatted … [127]
Deleted: 964
Deleted: 854
Formatted … [128]
Deleted: 842
Deleted: 876
Formatted … [129]
Formatted … [130]
Deleted: SWAP
Deleted: pH
Deleted: 0.307
Deleted: 0.299
Formatted … [131]
Deleted: 0.313
Deleted: 0.325
Deleted: 0.344
Deleted: Section Break (Next Page)
Formatted … [132]
Formatted … [133]
Formatted … [134]
Formatted … [135]
Formatted … [136]
Formatted … [137]
Formatted … [138]
Formatted … [139]
Formatted … [140]
Formatted … [141]
Formatted … [142]
Formatted … [143]
Formatted … [144]
Formatted … [145]
Formatted … [146]
Formatted … [147]
Formatted … [148]

Bond, G., Broecker, W., Johnsen, S., McManus, J., Labeyrie, L., Jouzel, J., and Bonani, G.: Correlations between climate records from North Atlantic sediments and Greenland ice, Nature, 365, 143–147, doi:10.1038/365143a0, 1993.

ter Braak, C. J. F. Partial canonical correspondence analysis. In: Classification and Related Methods of Data Analysis (ed. H. H. Bock), pp. 551-558. Elsevier Science Publishers B.V. (North-Holland) http://edepot.wur.nl/241165. 1988

ter Braak, C. J. F. and Barendregt, L. G.: Weighted averaging of species indicator values: Its efficiency in environmental calibration, Math Biosci, 78, 57–72, doi:10.1016/0025-5564(86)90031-3, 1986.

ter Braak, C. J. F. and te Beest, D. E. Testing environmental effects on taxonomic composition with canonical correspondence analysis: alternative permutation tests are not equal. Environ. Ecol. Stats, 29, 849–868. https://doi.org/10.1007/s10651-022-00545-4, 2022.

ter Braak, C. J. F. and Juggins, S.: Weighted averaging partial least squares regression (WA-PLS): an improved method for reconstructing environmental variables from species assemblages, Hydrobiologia 269, 485–502, doi:10.1007/BF00028046, 1993.

Brooks, S. J. and Birks, H. J. B.: Chironomid-inferred air temperatures from Lateglacial and Holocene sites in north-west Europe: progress and problems, Quat Sci Rev, 20, 1723–1741, doi:10.1016/S0277-3791(01)00038-5, 2001.

Bush, M. B., Correa-Metrio, A., van Woesik, R., Collins, A., Hanselman, J., Martinez, P., and McMichael, C. N. H.: Modern pollen assemblages of the Neotropics, J. Biogeogr., 48, 231–241, doi:10.1111/jbi.13960, 2021.

Christin, S., Hervet, É., Lecomte, N.: Applications for deep learning in ecology, Methods Ecol. Evol., 10, 1632–1644, doi:10.1111/2041-210X.13256, 2019.

Clapperton, C. M.: Maximum extent of the late Wisconsin glaciation in the Ecuadorian Andes, Quaternary of South America and Antarctic Peninsula, Balkema, Rotterdam, 165–180, doi: ISBN 9781003079323, 1987.

Cleator, S. F., Harrison, S. P., Nichols, N. K., Prentice, I. C., and Roulstone, I.: A new multivariable benchmark for Last Glacial Maximum climate simulations, Clim Past, 16, 699–712, doi:10.5194/cp-16-699-2020, 2020.

Colinvaux, P. A., Olson, K., and Liu, K. B.: Late-glacial and Holocene pollen diagrams from two endorheic lakes of the inter-Andean plateau of Ecuador, Rev. Palaeobot. Palynol., 55, 83–99, doi:10.1016/0034-6667(88)90055-3, 1988.

Colinvaux, P. A., Bush, M. B., Steinitz-Kannan, M., and Miller, M. C.: Glacial and Postglacial Pollen Records from the Ecuadorian Andes and Amazon, Quat. Res., 48, 69–78, doi:10.1006/qres.1997.1908, 1997.

Friedman J. H.: Greedy function approximation: A gradient boosting machine, Ann. Statist. 29(5), 1189–1232, doi:10.1214/aos/1013203451, 2011.

Geurts, P., Ernst, D., and Wehenkel, L.: Extremely randomized trees, Mach. Learn., 63, 3–42, doi:10.1007/s10994-006-6226-1, 2006.

Hais, M., Komprdová, K., Ermakov, N., and Chytrý, M.: Modelling the Last Glacial Maximum environments for a refugium of Pleistocene biota in the Russian Altai Mountains, Siberia, Palaeogeogr. Palaeoclimatol. Palaeoecol., 438, 135–145, doi:10.1016/j.palaeo.2015.07.037, 2015.

Formatted ... [262]
Formatted ... [263]
Formatted ... [264]
Formatted ... [265]
Formatted ... [266]
Formatted ... [267]
Formatted ... [268]
Formatted ... [269]
Formatted ... [270]
Formatted ... [271]
Moved down [2]: ter Braak. C. J. F. and Juggins, S.:
Formatted ... [272]
Formatted ... [273]
Formatted ... [274]
Formatted ... [275]
Formatted ... [277]
Formatted ... [276]
Moved (insertion) [2]
Deleted: Brook, B. W., Sodhi, N. S., and Bradshaw, C. ... [278]
Formatted ... [279]
Formatted ... [280]
Formatted ... [281]
Formatted ... [282]
Formatted ... [283]
Formatted ... [284]
Formatted ... [285]
Formatted ... [286]
Formatted ... [287]
Formatted ... [288]
Formatted ... [289]
Formatted ... [290]
Formatted ... [291]
Formatted ... [292]
Formatted ... [293]
Formatted ... [294]
Formatted ... [295]
Formatted ... [296]
Formatted ... [297]
Formatted ... [298]
Formatted ... [299]
Formatted ... [300]
Formatted ... [301]
Formatted ... [302]
Formatted ... [303]
Formatted ... [304]
Formatted ... [305]
Formatted ... [306]
Formatted ... [307]
Formatted ... [308]
Formatted ... [309]
Formatted ... [310]
Formatted ... [311]
Deleted: ,
Formatted ... [312]

Harrison, S. P: Modern pollen data for climate reconstructions, version 1 (SMPDS), University of Reading, doi: 10.17864/1947.194, 2019.

Harrison, S. P.: Climate reconstructions for the SMPDSv1 modern pollen data set, doi: 10.5281/zenodo.3605003, 2020.

Harrison, S. P., González-Sampériz, P., Gil-Romera, G.: Fossil pollen data for climate reconstructions from El Cañizar de Villarquemado, University of Reading, doi: 10.17864/1947.219, 2019.

Heiri, O., Lotter, A. F., Hausmann, S., and Kienast, F.: A chironomid-based Holocene summer air temperature reconstruction from the Swiss Alps, Holocene, 13, 477–484, doi:10.1191/0959683603hl640ft, 2003.

Helama, S., Makarenko, N. G., Karimova, L. M., Kruglun, O. A., Timonen, M., Holopainen, J., Meriläinen, J., and Eronen, M.: Dendroclimatic transfer functions revisited: Little Ice Age and Medieval Warm Period summer temperatures reconstructed using artificial neural networks and linear algorithms, Ann. Geophys., 27, 1097–1111, doi:10.5194/angeo-27-1097-2009, 2009.

Holden, P. B., Birks, H. J. B., Brooks, S. J., Bush, M. B., Hwang, G. M., Matthews-Bird, F., Valencia, B. G., and Van Woesik, R.: BUMPER v1.0: A Bayesian user-friendly model for palaeo-environmental reconstruction, Geosci. Model Dev., 10, 483–498, doi:10.5194/gmd-10-483-2017, 2017.

de la Houssaye, B., Flaming, P. L., Nixon, Q., and Acton, G. D.: Machine learning and deep learning applications for international ocean discovery program geoscience research, SMU Data Sci. Rev., 2(3), 9, https://scholar.smu.edu/datasciencereview/vol2/iss3/9, 2019.

Huang, Y., Yang, L. and Fu, Z.: Reconstructing coupled time series in climate systems using three kinds of machine-learning methods, Earth Syst. Dynam., 11, 835–853, doi:10.5194/esd-11-835-2020, 2020.

IBM, IBM360 infinitesimal jacknife, https://uq360.readthedocs.io/en/latest/extrinsic.html#infinitesimal-jackknife, 2024.

Jones, V. J., Stevenson, A. C., Battarbee, R. W.: Acidification of lakes in Galloway, south-west Scotland: a diatom and pollen study of the post-glacial history of the Round Loch of Glenhead, J. Ecol., 77, 1–22, doi:10.2307/2260912, 1989.

Jordan, G. J., Harrison, P. A., Worth, J. R. P., Williamson, G. J., and Kirkpatrick, J. B.: Palaeoendemic plants provide evidence for persistence of open, well-watered vegetation since the Cretaceous, Glob. Ecol. Biogeogr., 25, 127–140, doi:10.1111/geb.12389, 2016.

Juggins, S: Rioja: analysis of Quaternary science data, CRAN R package version (0.9–15.1), https://github.com/nsj3/rioja, 2017.

Ke, G., Meng, Q., Finley, T., Wang, T., Chen, W., Ma, W., Ye, Q., and Liu, T.-Y.: LightGBM: A highly efficient gradient boosting decision tree, in: I. Guyon, U. Von Luxburg, S. Bengio, H. Wallach, R. Fergus, S. Vishwanathan, and R. Garnett (eds) Advances in Neural Information Processing Systems, 30, 2017.

Liaw, A. and Wiener, M.: Classification and regression by randomForest, R news, 2(3), 18–22, http://www.stat.berkeley.edu/users/breiman/, 2002.

Formatted ... [415]
Formatted ... [417]
Formatted ... [418]
Formatted ... [419]
Formatted ... [416]
Formatted ... [420]
Formatted ... [421]
Moved (insertion) [5]
Formatted ... [422]
Formatted ... [423]
Formatted ... [424]
Formatted ... [425]
Formatted ... [426]
Formatted ... [427]
Formatted ... [428]
Formatted ... [429]
Formatted ... [430]
Formatted ... [431]
Formatted ... [432]
Formatted ... [433]
Formatted ... [434]
Formatted ... [435]
Formatted ... [436]
Formatted ... [437]
Moved up [5]: Climate reconstructions for the SMPDSv1
Moved up [4]: Hais, M., Komprdová, K., Ermakov, N., and
Deleted: Harrison, S.P.:
Deleted: Palaeoclimatol Palaeoecol, 438, 135–145, ... [449]
Formatted ... [438]
Formatted ... [439]
Formatted ... [440]
Formatted ... [441]
Formatted ... [442]
Formatted ... [443]
Formatted ... [444]
Formatted ... [445]
Formatted ... [446]
Formatted ... [447]
Formatted ... [448]
Formatted ... [450]
Formatted ... [451]
Formatted ... [452]
Formatted ... [453]
Formatted ... [454]
Formatted ... [455]
Formatted ... [456]
Formatted ... [457]
Formatted ... [458]
Formatted ... [459]
Formatted ... [460]
Formatted ... [461]
Formatted ... [462]
Formatted ... [463]
Formatted ... [464]

Liu, M., Prentice, I. C., ter Braak, C. J. **F., and** Harrison, S. P.**:** An improved statistical approach for reconstructing past climates from biotic assemblages, Proc. R. Soc. A, 476, **doi:10.1098/rspa.2020.0346,** 2020.

Norberg, A., Abrego, N., Blanchet, F. G., Adler, F. R., Anderson, B. J., Anttila, J., **Araújo**, M. B., Dallas, T., Dunson, D., Elith, J., Foster, S. D., Fox, R., Franklin, J., Godsoe, W., Guisan, A., **O'Hara**, B., Hill, N. A., Holt, R. D., Hui, F. K. C., Husby, M., **Kålås**, J. A., Lehikoinen, A., Luoto, M., Mod, H. K., Newell, G., Renner, I., Roslin, T., Soininen, J., Thuiller, W., Vanhatalo, J., Warton, D., White, M., Zimmermann, N. E., Gravel, D., **and** Ovaskainen, O.**:** A comprehensive evaluation of predictive performance of 33 species distribution models at species and community levels, **Ecol. Monogr.**, 89, **doi:10.1002/ecm.1370, 2019**,

Ovaskainen, O., Tikhonov, G., Norberg, A., Blanchet, F.G., Duan, L., Dunson, D., Roslin, T. & Abrego, N.: How to make more out of community data? A conceptual framework and its implementation as models and software, **Ecol. Lett. 20, 561-576**, doi:**10.1111/ele.12757, 2017**, 2017.

Paszke, A., Gross, S., Massa, F., Lerer, A., Bradbury, J., Chanan, G., **Killeen, T., Lin, Z., Gimelshein, N., Antiga, L. and Desmaison, A., Andreas K., Edward Z. Y., Zachary D., Martin R., Alykhan T., Sasank C., Benoit S., Lu F., Junjie B., and Soumith C.: Pytorch**: An **imperative style, high-performance deep learning library**, Advances in Neural Information Processing Systems, **32, 8024-8035, arXiv:1912.01703, 2019**,

Pedregosa, F., Varoquaux, G., Gramfort, A., Michel, V., Thirion, B., Grisel, O., Blondel, M., **Prettenhofer, P., Weiss, R., Dubourg, V., Vanderplas, J., Passos, A., Cournapeau, D., Brucher, M., Perrot, M., & Duchesnay, É.; Scikit-Learn: Machine Learning in Python. J. Mach. Learn. Res., 12, 2825–2830**, 2011.

Pennington, J., Socher, R**., and Manning, C.: GloVe: Global Vectors for Word Representation, in: Proceedings of the 2014 Conference on Empirical Methods in Natural Language Processing (EMNLP), 1532–1543, doi:10.3115/v1/D14-1162, 2014.**

Schulte, P.J. and **Hinckley, T.M.: A** comparison of pressure-volume curve data-analysis techniques, J. **Exp. Bot., 36, 1590–1602, doi: 10.1093/jxb/36.10.1590, 1985.**

Steinitz-Kannan M., Colinvaux P.A., Kannan R.**:** Limnological **Studies** in Ecuador 1. A survey **of** chemical and physical properties of Ecuadorian lakes, Arch. Hydrobiol., Suppl., 65, 61–105, 1983.

Stevenson, A. C, Juggins, S., Birks, H. J. B., Anderson, D. S., Anderson, N. J., Battarbee, R. W., Berge, F., Davis, R. B., Flower, R. J., and **Haworth, E. Y.: The Surface Waters Acidification Project Palaeolimnology Programme: Modern Diatom/Lake-Water Chemistry Data-Set, UCL Environmental Change Research Centre**, doi:**10.1098/rstb.1990.0056, 1991**,

Syam, N. and **Kaul, R.: Overfitting and Regularization in Machine Learning Models in Machine Learning and Artificial Intelligence in Marketing and Sales, Emerald Publishing Limited, Bingley, 65–84, doi: 10.1108/978-1-80043-880-420211004, 2021**

Telford, R.**, J. and Birks, H. J. B.:** A novel method for assessing the statistical significance of quantitative reconstructions inferred from biotic assemblages, **Quat.** Sci. Rev., 30, 1272–1278, doi:10.1016/j.quascirev.2011.03.002, 2011.

Deleted: Ter
Formatted ... [618]
Formatted ... [619]
Formatted ... [620]
Formatted ... [621]
Formatted ... [622]
Deleted: Proceedings of the Royal Society
Formatted ... [623]
Formatted ... [624]
Formatted ... [625]
Formatted ... [626]
Formatted ... [627]
Formatted ... [628]
Formatted ... [629]
Formatted ... [630]
Formatted ... [631]
Formatted ... [632]
Formatted ... [633]
Formatted ... [634]
Formatted ... [635]
Formatted ... [636]
Formatted ... [637]
Formatted ... [638]
Formatted ... [639]
Formatted ... [640]
Formatted ... [641]
Formatted ... [642]
Formatted ... [643]
Formatted ... [644]
Formatted ... [645]
Formatted ... [646]
Formatted ... [647]
Formatted ... [648]
Formatted ... [649]
Formatted ... [650]
Formatted ... [651]
Formatted ... [652]
Formatted ... [653]
Formatted ... [654]
Formatted ... [655]
Formatted ... [656]
Formatted ... [657]
Formatted ... [658]
Formatted ... [659]
Formatted ... [660]
Formatted ... [661]
Formatted ... [662]
Deleted: ,
Formatted ... [663]
Formatted ... [664]
Formatted ... [665]
Moved down [8]: Pedregosa, F., Varoquaux, G., Gramfort, A.,
Formatted ... [666]
Formatted ... [667]

Telford, R. J. and Trachsel, M.: palaeoSig: Significance Tests for Palaeoenvironmental Reconstructions. R Package Version 1.1-3. Bergen: University of Bergen, 2015.

Turner, M. G., Wei, D., Prentice, I. C., and Harrison, S. P.: The impact of methodological decisions on climate reconstructions using WA-PLS, Quat. Res., 99, 341–356, doi:10.1017/qua.2020.44, 2020.

Urrego, D. H., Bush, M. B., and Silman, M. R.: A long history of cloud and forest migration from Lake Consuelo, Peru, Quat. Res., 73, 364–373, doi:10.1016/j.yqres.2009.10.005, 2010.

Wei, D., González-Sampériz, P., Gil-Romera, G., Harrison, S. P., and Prentice, I. C.: Seasonal temperature and moisture changes in interior semi-arid Spain from the last interglacial to the Late Holocene, Quat. Res., 101, 143–155, doi:10.1017/qua.2020.108, 2021a.

Wei, G., Peng, C., Zhu, Q., Zhou, X., and Yang, B.: Application of machine learning methods for paleoclimatic reconstructions from leaf traits, Int. J. Clim., 41, E3249–E3262, doi:10.1002/joc.6921, 2021b.

Yates, L. A., Aandahl, Z., Richards, S. A., and Brook, B. W.: Cross validation for model selection: A review with examples from ecology, Ecol. Monogr., 93, doi:10.1002/ecm.1557, 2023.

Yeom, S., Giacomelli, I., Fredrikson, M. & Jha, S.: Privacy Risk in Machine Learning: Analyzing the Connection to Overfitting, 2018 IEEE 31st Computer Security Foundations Symposium (CSF), 268-282, doi:10.1109/CSF.2018.00027, 2018.

Zhou, Z. H.: Ensemble Methods: Foundations and Algorithms, 236, CRC Press, New York, ISBN 9780429151095, 2012.

Moved (insertion) [10]
Moved (insertion) [11]
Formatted ... [743]
Formatted ... [745]
Formatted ... [746]
Formatted ... [747]
Formatted ... [744]
Formatted ... [748]
Formatted ... [749]
Formatted ... [750]
Formatted ... [751]
Formatted ... [752]
Formatted ... [753]
Formatted ... [754]
Formatted ... [755]
Formatted ... [756]
Formatted ... [757]
Deleted: ,
Formatted ... [758]
Formatted ... [759]
Formatted ... [760]
Formatted ... [761]
Formatted ... [762]
Formatted ... [763]
Formatted ... [764]
Deleted: Tylianakis, J. M., Didham, R. K., Bascompte, ... [765]
Formatted ... [766]
Formatted ... [767]
Formatted ... [768]
Formatted ... [769]
Formatted ... [770]
Formatted ... [771]
Formatted ... [772]
Formatted ... [773]
Formatted ... [774]
Formatted ... [775]
Formatted ... [776]
Formatted ... [777]
Deleted: ,
Formatted ... [778]
Formatted ... [779]
Formatted ... [780]
Formatted ... [781]
Formatted ... [782]
Formatted ... [783]
Formatted ... [784]
Formatted ... [785]
Formatted ... [786]
Formatted ... [787]
Formatted ... [788]
Formatted ... [789]
Formatted ... [790]
Formatted ... [791]
Deleted: ,

Page 3: [1] Deleted	Phil Holden	13/05/2024 10:30:00

Page 11: [2] Formatted	Philip.Holden	13/05/2024 10:30:00

Centred

Page 11: [3] Formatted	Philip.Holden	13/05/2024 10:30:00

Font: 10 pt

Page 11: [4] Formatted	Philip.Holden	13/05/2024 10:30:00

Font: 10 pt

Page 11: [5] Formatted	Philip.Holden	13/05/2024 10:30:00

Font: 10 pt

Page 11: [6] Formatted	Philip.Holden	13/05/2024 10:30:00

Font: 10 pt

Page 11: [7] Formatted	Philip.Holden	13/05/2024 10:30:00

Font: 10 pt

Page 11: [8] Formatted	Philip.Holden	13/05/2024 10:30:00

Font: 10 pt

Page 11: [9] Formatted	Philip.Holden	13/05/2024 10:30:00

Font: 10 pt

Page 11: [10] Formatted	Philip.Holden	13/05/2024 10:30:00

Centred

Page 11: [11] Formatted Table	Philip.Holden	

Formatted Table

Page 11: [12] Formatted	Philip.Holden	13/05/2024 10:30:00

Font: 10 pt

Page 11: [13] Formatted	Philip.Holden	13/05/2024 10:30:00

Font: 10 pt

Page 11: [14] Formatted	Philip.Holden	13/05/2024 10:30:00

Font: 10 pt

Page 11: [15] Formatted	Philip.Holden	13/05/2024 10:30:00

Font: 10 pt

Page 11: [16] Formatted	Philip.Holden	13/05/2024 10:30:00

Font: 10 pt

Page 11: [17] Formatted	Philip.Holden	13/05/2024 10:30:00